Journal of Nuclear Medicine, published on April 16, 2021 as doi:10.2967/jnumed.120.256719

Patient Size-Dependent Dosimetry Methodology Applied to ^{18}F-FDG Using New ICRP Mesh Phantoms

Running title: Patient-dependent FDG dosimetry

Authors: Lukas M. Carter[1], Chansoo Choi[2], Simone Krebs[3], Bradley J. Beattie[1], Chan Hyeong Kim[2], Heiko Schoder[3], Wesley E. Bolch[4], Adam L. Kesner[1]

Affiliations:

[1]Department of Medical Physics, Memorial Sloan Kettering Cancer Center, New York, NY, USA

[2]Department of Nuclear Engineering, Hanyang University, Seoul, Republic of Korea

[3]Department of Radiology, Memorial Sloan Kettering Cancer Center, New York, NY, USA

[4]J. Crayton Pruitt Department of Biomedical Engineering, University of Florida, Gainesville, FL, USA

Correspondence:

Lukas M. Carter

Department of Medical Physics, MSKCC
1250 1st Avenue, New York, NY, 10065, USA
carterl1@mskcc.org
ORCiD: https://orcid.org/0000-0003-4848-4190

Keywords: FDG; patient-dependent dosimetry, PARaDIM, PHITS, phantom

ABSTRACT

Despite the known influence of anatomic variability on internal dosimetry, dosimetry for ^{18}F-FDG and other diagnostic radiopharmaceuticals is routinely derived using *reference* phantoms, which embody population-averaged morphometry for a given age and sex. Moreover, phantom format affects dosimetry estimates to varying extent. Here, we applied newly developed mesh format reference phantoms and a *patient-dependent* phantom library to assess the impact of height, weight, and body contour variation on dosimetry of ^{18}F-FDG. We compared the mesh reference phantom dosimetry estimates with corresponding estimates from common software to identify differences related to phantom format or software implementation. Our study serves as an example of how more precise patient size-dependent dosimetry methodology could be performed.

Methods: Absorbed dose coefficients were computed for the adult mesh reference phantoms and derivative patient-dependent phantom series by Monte Carlo simulation using the PHITS radiation transport code within PARaDIM software. The dose coefficients were compared with reference absorbed dose coefficients obtained from ICRP Publication 128, or generated using software including OLINDA 2.1, OLINDA 1.1, and IDAC-dose 2.1.

Results: Differences in dosimetry arising from anatomical variations were shown to be significant, with detriment-weighted dose coefficients for the percentile-specific phantoms varying by up to ±40% relative to the corresponding reference phantom effective dose coefficients, irrespective of phantom format. Similar variations were seen in the individual organ absorbed dose coefficients for the percentile-specific phantoms relative to the reference phantoms. The effective dose coefficient for the mesh reference adult was 0.017 mSv/MBq, which was 5% higher than estimated by a corresponding voxel phantom, and 10% lower than estimated by the stylized phantom format.

Conclusions: We observed notable variability in ^{18}F-FDG dosimetry across morphometrically different patients, supporting the use of patient-dependent phantoms for more accurate dosimetric estimations relative to standard reference dosimetry. These data may help in optimizing imaging protocols and research studies, in particular when longer-lived isotopes are employed.

INTRODUCTION

2-Deoxy-2-[^{18}F]fluoroglucose (^{18}F-FDG) is the most widely used diagnostic radiopharmaceutical in oncology, with 2.2 million clinical PET scans performed across U.S. facilities in 2019(*1*). The typical effective dose from ^{18}F-FDG imaging is ~10mSv and is considered low(*2*,*3*). Nevertheless, the increasing use of radiation-based medical imaging over the past several decades has led to concerns about possible detriment, which have precipitated campaigns such as *Image Wisely* (adult patients) and *Image Gently* (pediatric patients)(*4*,*5*). A cornerstone of those campaigns is attention to optimization. Accurate dosimetry is fundamental to understanding relationships between radiation dose and patient detriment and is needed to provide objective recommendations for administered activity for different patient populations(*6*).

Dosimetry estimates in nuclear medicine are derived using Monte Carlo-based dose calculations incorporating computerized representations of anatomy known as computational phantoms. The accuracy of these estimates depends on the degree to which anatomical features of the patient are modelled within the phantom. Virtually all routine dosimetry estimates for ^{18}F-FDG in adult patients have utilized standard *reference* (i.e. non patient-specific) phantoms to represent patient anatomy. Reference phantoms serve to define an "average patient" based on only age and sex criteria; they do not consider differing body sizes and organ dimensions, which may influence absorbed dose calculations by 20-60%(*7*). The geometric format (e.g. mesh, voxel, stylized, or hybrid) used to define the phantom anatomy further influences dose calculations. Despite the availability of more modern formats, stylized adult phantoms(*8*,*9*) as described in ICRP 23(*10*) continue to be routinely used in nuclear medicine dosimetry software, and provide the underpinning for dose coefficients promulgated in current accepted sources of radiopharmaceutical reference data(*11*). Limitations of stylized phantoms include reliance on simple linear and quadratic surface equations, which coarsely approximate human anatomy and generally underestimate organ cross-dose contributions for low energy photons. Progress in computational phantom and Monte Carlo code development (*12–19*) now enable more accurate dosimetry protocols, which will support dosimetry research, optimization of clinical imaging protocols, and planning of research studies.

The ICRP recently developed mesh format reference computational phantoms (MRCPs) for the adult male and female, which provide anatomically more realistic representations of the human body (Figure 1)(*20*). For example, these phantoms define numerous additional source and target regions, and define small, thin, or complex radiosensitive target regions impractical to treat using voxel or stylized phantom formats. More recently, the adult mesh reference phantoms were re-shaped and scaled to match Caucasian patient population-dependent parameters extracted from anthropometric survey data (*21*,*22*) — culminating in an additional 9 male and 9 female phantoms representing the 10th, 50th, and 90th percentiles of standing height and weight for the adult Caucasian population. Termed the "percentile-specific" phantom series, these 18 phantoms are morphometrically considered *patient-dependent* phantoms and foster

research into dosimetric implications of adult patient size variability across population subsets.(*23*)

A primary objective of this work was to assess differences in ^{18}F-FDG dose coefficient estimations using a patient-dependent dosimetry paradigm, in comparison to standard "one-size-fits-all" reference dosimetry. We therefore calculated dosimetry estimates across a series of current-generation mesh patient dependent phantoms to evaluate the differences arising from anatomical variability. We also investigated differences due to phantom format by comparing dose coefficients derived using the mesh reference phantoms with those obtained using stylized reference phantoms, voxel reference phantoms, or hybrid reference phantoms.

MATERIALS AND METHODS

Biokinetic Data for ^{18}F-FDG

Biokinetic data for ^{18}F-FDG, in the form of time-integrated activity coefficients (TIACs)(*24*) for the brain, heart wall, lungs, liver, urinary bladder contents, and rest of body, were obtained from the ICRP 128(*11*) radiopharmaceutical data compendium (Table 1). The TIAC for the lung region provided in ICRP 128 applies to both lungs jointly; however, in the mesh phantoms, the lungs are modeled as separate regions, with each requiring an input TIAC. Therefore, the lung TIAC was divided between the right and left lung regions by mass fraction (relative to the total lung mass). Similarly, the rest of body TIAC was divided among its comprising regions by tissue mass fraction (relative to the total tissue mass of the rest of body).

Absorbed Dose Dalculations with Reference and Patient-Dependent Mesh Phantoms

Absorbed dose coefficients (in units of mGy/MBq administered activity) for the explicitly defined mesh reference and percentile-specific phantom regions were computed by direct Monte Carlo simulation using the PHITS-based(*15*) PARaDIM software(*18*). Each simulation was configured using the "multi-source" absorbed dose mode of PARaDIM, which generates both region-level mean absorbed dose coefficients as well as a 3D voxelized dose map (here, sampled at 1.0 cm isotropic spatial resolution). The material surrounding the phantom was defined as void. A total of 10^7 histories were simulated for each phantom. PARaDIM defaults for physical models were used, which specified the PHITS-EGS5 method for treatment of multiple scattering, explicit treatment of fluorescent x-rays, consideration of Rayleigh and incoherent scattering, and consideration of electron-impact ionization. Sampling was utilized for determination of bremsstrahlung polar angles, pair electron polar angles, and distribution of photoelectrons. Cutoff energies of 1.0 keV were utilized for both positrons and photons.

The ICRP defines several target regions that comprise multiple uniquely defined target regions within the phantoms (e.g. lungs, comprising left and right lung; kidneys,

comprising left and right renal pelvis, cortex, and medulla). The mean dose to such regions was computed as a mass-weighted combination of absorbed doses to each subregion:

$$d_{mreg} = \sum_{r_T \in mreg} \frac{M(r_T \in mreg)}{M(mreg)} d(r_T \in mreg) \quad \text{Eqn. 1}$$

where d_{mreg} is the absorbed dose coefficient for a multi-region target $mreg$; $M(r_T \in mreg)$ is the mass of a region r_T comprising the multi-region target; $M(mreg)$ is the total mass of the multi-region target; and $d(r_T \in mreg)$ is the absorbed dose coefficient for a subregion.

The active marrow and endosteum are implicitly defined within the spongiosa and marrow cavity regions of the mesh reference and percentile-specific phantoms; the absorbed dose coefficients for these specific tissues was derived from those for the corresponding spongiosa and marrow cavities per the recommendations in ICRP 116, *viz*:

$$d_{skel}(AM) = \sum_{r_T \in skel} \frac{M(AM, r_T \in skel)}{M(AM)} d(SP, r_T \in skel) \quad \text{Eqn. 2}$$

$$d_{skel}(EC) = \sum_{r_T \in skel} \frac{M(EC, r_T \in skel)}{M(EC)} d(SP, r_T \in skel) + \sum_{r_T} \frac{M(EC, r_T \in skel)}{M(EC)} d(MM, r_T \in skel) \quad \text{Eqn. 3}$$

where $d_{skel}(AM)$ and $d_{skel}(EC)$ are the skeletal-averaged absorbed dose coefficients for the active marrow and endosteal cells, respectively; $M(AM, r_T \in skel)$ and $M(EC, r_T \in skel)$ are the masses of these tissues in skeletal target region $r_T \in skel$; $M(AM)$ and $M(EC)$ are the total masses of active marrow and endosteal cells contained within the entire skeleton; and $d(SP, r_T \in skel)$ and $d(MM, r_T \in skel)$ are the absorbed dose coefficients for the spongiosa and medullary marrow regions which encompass the active marrow and endosteal cells in skeletal region r_T.

The effective dose quantity is derived from absorbed dose calculations and is a widely used concept in diagnostic radiation dosimetry – is provides a strategy for combining the variable organ doses into a single stochastic risk-relevant number(*25*,*26*,*27*). Effective dose coefficients(*28*) were computed using the methodology and tissue-specific weighting factors promulgated in ICRP 103 and ICRP 133, *viz*:

$$e = \sum_T w_T \sum_R w_R \left[\frac{d_{T,R}^{male} + d_{T,R}^{female}}{2} \right] \quad \text{Eqn. 4}$$

where e is the effective dose coefficient, w_T is the tissue-specific weighting factor for tissue T, and w_R is the radiation weighting factor for radiation type R (here, taken as unity for ^{18}F positrons and photons).

By definition, the effective dose is relevant only for the reference person (i.e. it does not formally apply to height, weight or otherwise constrained subsets of the patient population)(*24*,*25*). It is also restricted to the use of sex-averaged organ absorbed doses as per Eqn. 4. To gain insight into an similar single-value risk characterization, a related quantity, the *detriment weighted dose* (*29–31*) has been previously introduced which applies ICRP tissue and radiation weighting factors, but removes the requirement of sex-

averaging of organ absorbed doses, as well as the restriction of non-reference phantom dose values. The detriment-weighted dose provides a basis for consideration of risk from stochastic effects of radiation, as relevant to population subsets (as used here) or potentially individuals, and is used with the justification that absorbed dose, not patient geometry, is the relevant seat for quantifying risk:

$$e_{DW}^{S,H,M} = \sum_T w_T \sum_R w_R d_{T,R}^{S,H,M} \quad \text{Eqn. 5}$$

where $e_{DW}^{S,H,M}$ is the detriment-weighted dose coefficient for a phantom of sex S, height H, and total body mass M.

Absorbed Dose Calculations with Reference Voxel, Stylized, and Hybrid Phantoms

The "ICRP 89 adult" male and female hybrid reference phantoms(*19*) were utilized in OLINDA 2.1. The adult male and female stylized reference phantoms were utilized in OLINDA 1.1, and the ICRP 110 adult voxel reference phantoms were used in IDAC-dose 2.1 software. The default organ masses were used for each phantom in all software. For further details on the phantoms used, please refer to Table 2.

Hardware and Software Specification

An HP Z8 workstation running Microsoft Windows 10 operating system and utilizing a 3.6-GHz Intel Xeon 5122 processor, was used for all Monte Carlo calculations.

3D Slicer (version 4.11; www.slicer.org) was used for dose map visualization, and Paraview (version 5.6.2; www.paraview.org) was used for 3D rendering of phantom geometry. Statistical analysis was performed with GraphPad Prism (version 8.3.1; GraphPad Software, Inc.).

RESULTS

Figure 2 shows voxel-level absorbed dose coefficients for the mesh reference and percentile-specific phantom series. These 3D dose maps are volume-rendered as maximum intensity projections, and as they were derived under the assumption of uniformly distributed activity within whole organs, they are intended to reflect spatial nonuniformity of dose deposition averaged across a patient subpopulation matching the specified height and weight. Region-level mean absorbed dose coefficients for selected target organs of the phantoms are presented in Figure 3 and Figure 4. A comprehensive list of dose coefficients for all defined target regions is provided in Supplemental Tables S1-8. The highest absorbed dose coefficients were observed in the heart wall, followed by the urinary bladder wall, and brain, for the male and female mesh phantoms and their voxel analogs implemented in IDAC-dose 2.1 (Figure 5). In contrast, the urinary bladder wall was identified as the critical organ in the stylized and hybrid reference phantom

dose estimates, with the bladder wall absorbed dose coefficients being approximately two-fold higher than those for the heart wall (the next most-irradiated tissue), and were approximately 2.5-fold higher than estimated with the mesh reference phantoms. This discrepancy has been noted previously(*18*), and here, was the largest relative deviation in the dose coefficient estimated by the mesh reference phantoms in comparison to the corresponding stylized and hybrid phantom estimates. The disagreement can be partially explained by the methodology employed for determination of specific absorbed fractions used in derivation of self-irradiation S-values (and correspondingly, absorbed dose coefficients) for the urinary bladder of the stylized phantoms(*32*,*33*). Absorbed dose coefficients for the basal cell layer of the urinary bladder of the mesh reference adults (0.089 mGy/MBq and 0.091 mGy/MBq for adult male and female, respectively; Supplemental Table S1-2) were more consistent with the stylized and hybrid phantom bladder dose estimates.

Relative to the reference mesh phantoms of the corresponding sex, absorbed dose coefficients for most target organs of the percentile-specific phantom series deviated by 20-30% for the 10^{th} and 90^{th} weight percentile extremes. The reference and percentile-specific estimates converged near the H50 / W50 percentile classification; this was expected due to the similar body morphometry of the reference phantoms (176.0 cm / 73 kg male; 163 cm / 60.0 kg female) and the H50 / W50 analogs (176.5 cm / 79.3 kg male; 163.3 cm / 64.1 kg female). Of all target tissues, absorbed dose coefficients for the brain varied the least (in relative terms) among phantoms of the same sex, primarily due to the weak dependence of brain mass on body morphometry – particularly body mass for a given height.

The effective dose coefficient was calculated as 0.017 mSv/MBq, using the male and female mesh reference phantoms in combination with the tissue-specific weighting factors of ICRP 103. This represents a ~10% decrease relative to ICRP 128 estimate of 0.019 mSv/MBq and reflects geometric differences in the phantoms, tissue-specific weighting factors (Table 2), and lack of sex-averaging the ICRP 128 organ doses used to derive the effective dose. The effective dose coefficient for the ICRP 110 voxel phantoms was 0.016 mSv/MBq (sex-averaged) which agrees within ~5% with the mesh reference phantom estimates; of note, these phantoms were designed to represent identical geometry, but in different formats.

The detriment-weighted dose coefficient for each of the percentile-specific phantoms was computed by applying ICRP 103 tissue-specific weighting factors directly to the associated tissue equivalent dose coefficients (i.e. not using reference male/female equivalent dose averaging; see Eqn. 5). The patient-dependence of the detriment-weighted dose is provided in Figure 6 for the percentile-specific phantoms. Though the relationships depend on height, weight, sex, and underlying physical factors (linear energy transfer, attenuation), the detriment-weighted dose is strongly negatively correlated with body mass (Spearman's r = -0.9505; p < 0.0001), but less strongly with BMI (Spearman's r = -0.7049; p = 0.0011). Notably, given a particular sex, the detriment-weighted dose vs. mass curves for different height classifications were observed to

decrease monotonically. For a given mass, detriment-weighted dose coefficients for females were larger than for males. Together these results suggest that consideration of body morphometry, rather than only body mass, will further improve dose estimates and optimization strategies.

DISCUSSION

Diagnostic dose measurement has roles in optimization, comparing techniques and modalities, quality assurance, research and development, and support of regulatory standards and public health protection.(*25*) Understanding the variability and uncertainty in dose estimates is of heightened importance considering repeat oncologic imaging sessions where uncertainties must be propagated across multiple imaging sessions throughout disease management. The contributing factors for uncertainty in organ-level absorbed dose calculations (*34–36*) can include uncertainty in: 1) radionuclide physical decay data, 2) system calibration, 3) Monte Carlo calculation of energy deposition, 4) body morphometry of the patient in comparison to the phantom representing the patient, 5) radiopharmaceutical biokinetics and intra-organ distribution. Of these, the uncertainty in radionuclide decay data is negligible in most cases, and uncertainty in Monte Carlo simulations can be minimized with adequate sampling. In contrast, body morphometry and radiopharmaceutical biokinetics and intra-organ distribution represent the principal organ-level dosimetric uncertainties.

Our study addresses uncertainty and variability in body morphometry for specific subsets of the Caucasian patient population, and we provide *patient-dependent* dose estimates (with a broad approximation of the anatomy of height- and weight-defined subsets of the patient population), in contrast to *patient-specific* calculations (which account for the unique anatomy of a specific patient)(*23*). In doing so, we have utilized reference ^{18}F-FDG biokinetic data in order to ensure the variability in the results originates plainly from the underlying anatomical differences. The biokinetics of ^{18}F-FDG may vary across patients, for instance due to dietary conditions, presence of tumors, and kidney dysfunction. To our knowledge, the biokinetic dependence on adult body morphometry has not been comprehensively investigated. Considering the uncertainty in biokinetics, as well as the impracticality of creating patient-specific phantoms for routine imaging procedures, there is some rationale for applying these dose estimates to specific patients by matching them to the appropriate height and weight percentiles. Such strategies could support scan-specific dose reporting in nuclear medicine in the near future.

Role of Patient-Dependent Dose Coefficients in Diagnostic Nuclear Medicine

Optimization strategies for FDG should continue to prioritize the delivery of diagnostic quality images. The *Image Wisely* and *Image Gently* initiatives(*4*,*5*) espouse safe and efficacious imaging by striving to deliver diagnostic quality images while maintaining radiation doses as low as reasonably achievable. Our calculations provide

supporting data for patient size-based ^{18}F-FDG administration and related optimization strategies. At ^{18}F-FDG dose levels expected clinically, the confidence intervals in risk-dose relationships are currently too broad to justify the consideration of risk in management of individual patients(*37*,*38*). Therefore, the dose coefficients we have provided should be used primarily for improved scan-specific dose reporting, which will enable better elucidation of dose-risk relationships in epidemiologic studies. Incorporating patient size-dependent variation in ^{18}F-FDG biokinetics would allow further refinement of the present dose coefficient estimates and would allow them to be more confidently used in setting guidelines for administered activity as a function of adult body morphometry. A greater impact of morphometry-dependent variation in absorbed dose and detriment-weighted dose coefficients can be expected with longer half-life diagnostic radiopharmaceuticals.

Methodological Considerations

In contrast with the orthodox method of computing dose coefficients from specific absorbed fraction-derived S-value lookup tables, here, we have computed task-specific dose coefficients via direct Monte Carlo simulation. The derivation of a complete set of phantom organ specific absorbed fractions requires a monumental computational effort. For example, ICRP 133 provides specific absorbed fractions for the ICRP 110-series adult phantoms, for 79 unique source regions, across three corpuscular radiation types plus photons, and ~20 discrete energies necessary for interpolation – effectively requiring over 6,000 individual Monte Carlo simulations per phantom – but thereafter enabling dose from any radionuclide/biokinetic dataset to be immediately computed. For the direct approach used here, a single phantom requires a new Monte Carlo simulation for every biokinetic dataset, but the simulation can be run on a standard desktop computer on a clinically acceptable timescale. Thus, future availability of specific absorbed fractions for the mesh reference and percentile specific phantoms will increase flexibility and computation speed, but their current unavailability should not present a barrier to implementation of these phantoms.

Some organ-level dosimetry software, including OLINDA, allow users to modify reference phantom organ masses to approximate patient-specific dose calculations. These approaches typically involve linearly scaling the self-S contributions from weakly penetrating radiations (alpha particles and electrons) with inverse mass, while photon self-S contributions are scaled inversely with the 2/3 power of the mass(*33*). This approach assumes that source-target proximity is invariant upon changes in organ mass or patient shape. This approach is reasonable when the phantom already recapitulates the salient morphometry of the patient or patient population subset (e.g. for small mass variation in larger spheriform organs), but may be subject to considerable errors when, for example, scaling reference phantom S-values to match patients of much smaller or much larger overall size. As the percentile-specific phantoms account for gross size variation across patients, they would serve as a better basis for patient-specific organ S-value scaling.

CONCLUSION

Using newly developed computational phantoms, we provide patient-dependent dose coefficients and revised reference dose coefficients for ^{18}F-FDG. Of note, differences in patient morphometry imparted large deviations in dose coefficients for the upper and lower 10th percentile extremes of patient height and weight (up to ± 40% relative to the reference patient). While our work was limited to ^{18}F-FDG, greater impact is expected for longer-lived isotopes in imaging. These data pertain to stochastic risk estimates and should not be used for individual patient management, but the methodology described may support optimization of administered activities in clinical practice.

ACKNOWLEDGEMENTS

This research was funded in part through the NIH/NCI Cancer Center Support Grant P30 CA008748 and NIH U01 EB028234. L.M.C acknowledges support from the Ruth L. Kirschstein NRSA Postdoctoral Fellowship (NIH F32 EB025050). S.K. was supported in part by the NIH/NCI Paul Calabresi Career Development Award for Clinical Oncology (K12 CA184746). We are enormously grateful for technical support from the PHITS team of the Japanese Atomic Energy Administration, including Dr. Tatsuhiko Sato and Dr. Takuya Furuta. No other potential conflict of interest relevant to this article was reported.

KEY POINTS

Question: Can the influence of patient size on ^{18}F-FDG dosimetry be elucidated using - newly-developed patient-dependent phantoms?

Pertinent findings: Dose coefficients for ^{18}F-FDG were shown to vary by up to ± 40% across the 10th – 90th percentiles for standing height and weight across the Caucasian adult patient population.

Implications for patient care: Implementation of the current state-of-the-art phantom libraries into modernized dosimetry software will foster greater accuracy in dosimetry and ultimately support optimized strategies for personalized nuclear medicine.

REFERENCES

1. 2020 PET imaging market summary report. *Int Mark Ventur*. 2020.

2. Council NR, Studies D on E and L, Research B on RE, Radiation C to AHR from E to LL of I. Health risks from exposure to low levels of ionizing radiation: BEIR VII Phase 2. National Academies Press; 2006.

3. Vetter RJ. ICRP Publication 103, The recommendations of the international commission on radiological protection. *Health Phys*. 2008;95:445.

4. Brink JA, Amis ES. Image Wisely: A Campaign to increase awareness about adult radiation protection. *Radiology*. 2010;257:601-602.

5. Applegate KE, Cost NG. Image Gently: A campaign to reduce children's and adolescents' risk for cancer during adulthood. *J Adolesc Health*. 2013;52:S93-S97.

6. Sgouros G, Frey EC, Bolch WE, Wayson MB, Abadia AF, Treves ST. An approach for balancing diagnostic image quality with cancer risk: application to pediatric diagnostic imaging of 99mTc-dimercaptosuccinic acid. *J Nucl Med*. 2011;52:1923-1929.

7. Mattsson S, Johansson L, Leide Svegborn S, et al. Radiation dose to patients from radiopharmaceuticals: a compendium of current information related to frequently used substances. *Ann ICRP*. 2015;44:7-321.

8. Cristy M, Eckerman KF. Specific absorbed fractions of energy at various ages from internal photon sources: 7, Adult male. Oak Ridge National Lab.; 1987.

9. Snyder WS, Fisher HL, Ford MR, Warner GG. Estimates of absorbed fractions for monoenergetic photon sources uniformly distributed in various organs of a heterogeneous phantom. *J Nucl Med Off Publ Soc Nucl Med*. August 1969:Suppl 3:7-52.

10. ICRP Publication 23. *SAGE Publ Ltd*. October 2020.

11. Mattsson S, Johansson L, Leide Svegborn S, et al. Radiation dose to patients from radiopharmaceuticals: a compendium of current information related to frequently used substances. *Ann ICRP*. 2015;44:7-321.

12. Zubal IG, Harrell CR, Smith EO, Rattner Z, Gindi G, Hoffer PB. Computerized three-dimensional segmented human anatomy. *Med Phys*. 1994;21:299-302.

13. Zaidi H, Xu XG. Computational anthropomorphic models of the human anatomy: the path to realistic Monte Carlo modeling in radiological sciences. *Annu Rev Biomed Eng*. 2007;9:471-500.

14. Geyer AM, O'Reilly S, Lee C, Long DJ, Bolch WE. The UF/NCI family of hybrid computational phantoms representing the current US population of male and female

children, adolescents, and adults—application to CT dosimetry. *Phys Med Biol*. 2014;59:5225-5242.

15. Sato T, Iwamoto Y, Hashimoto S, et al. Features of Particle and Heavy Ion Transport code System (PHITS) version 3.02. *J Nucl Sci Technol*. 2018;55:684-690.

16. Furuta T, Sato T, Han MC, et al. Implementation of tetrahedral-mesh geometry in Monte Carlo radiation transport code PHITS. *Phys Med Biol*. 2017;62:4798.

17. Agostinelli S, Allison J, Amako K, et al. Geant4—a simulation toolkit. *Nucl Instrum Methods Phys Res Sect Accel Spectrometers Detect Assoc Equip*. 2003;506:250-303.

18. Carter LM, Crawford TM, Sato T, et al. PARaDIM – A PHITS-based Monte Carlo tool for internal dosimetry with tetrahedral mesh computational phantoms. *J Nucl Med*. June 2019:jnumed.119.229013.

19. Stabin MG, Xu XG, Emmons MA, Segars WP, Shi C, Fernald MJ. RADAR reference adult, pediatric, and pregnant female phantom series for internal and external dosimetry. *J Nucl Med*. 2012;53:1807-1813.

20. Kim CH, Yeom YS, Petoussi-Henss N, et al. ICRP Publication 145: Adult mesh-type reference computational phantoms. *Ann ICRP*. 2020;49:13-201.

21. Cassola VF, Milian FM, Kramer R, Lira CAB de O, Khoury HJ. Standing adult human phantoms based on 10th, 50th and 90th mass and height percentiles of male and female Caucasian populations. *Phys Med Biol*. 2011;56:3749-3772.

22. Lee H, Yeom YS, Nguyen TT, et al. Percentile-specific computational phantoms constructed from ICRP mesh-type reference computational phantoms (MRCPs). *Phys Med Biol*. January 2019.

23. Bolch W, Lee C, Wayson M, Johnson P. Hybrid computational phantoms for medical dose reconstruction. *Radiat Environ Biophys*. 2010;49:155-168.

24. Bolch WE, Eckerman KF, Sgouros G, Thomas SR. MIRD pamphlet No. 21: a generalized schema for radiopharmaceutical dosimetry--standardization of nomenclature. *J Nucl Med Off Publ Soc Nucl Med*. 2009;50:477-484.

25. Martin CJ, Harrison JD, Rehani MM. Effective dose from radiation exposure in medicine: Past, present, and future. *Phys Med*. 2020;79:87-92.

26. Harrison JD, Balonov M, Bochud F, et al. ICRP Publication 147: Use of dose quantities in radiological protection. *Ann ICRP*. 2021;50:9-82.

27. Harrison JD, Balonov MI, Bochud FO, et al. The use of dose quantities in radiological protection: ICRP Publication 147 Ann ICRP 50(1) 2021. *J Radiol Prot*. 2021.

28. Bolch WE, Jokisch D, Zankl M, et al. ICRP Publication 133: The ICRP computational framework for internal dose assessment for reference adults: specific absorbed fractions. *Ann ICRP*. 2016;45:5-73.

29. Kofler C, Domal S, Satoh D, Dewji S, Eckerman K, Bolch WE. Organ and detriment-weighted dose rate coefficients for exposure to radionuclide-contaminated soil considering body morphometries that differ from reference conditions: adults and children. *Radiat Environ Biophys*. 2019;58:477-492.

30. Brown J, Sexton-Stallone B, Li Y, et al. Body morphometry appropriate computational phantoms for dose and risk optimization in pediatric renal imaging with Tc-99m DMSA and Tc-99m MAG3. *Phys Med Biol*. 2020.

31. Brown J, Sexton-Stallone B, Li Y, et al. Dosimetric considerations of Tc-99m MDP uptake within the epiphyseal plates of the long bones of pediatric patients. *Phys Med Biol*. 2020.

32. Stabin MG. MIRDOSE: Personal computer software for internal dose assessment in nuclear medicine. *J Nucl Med*. 1996;37:538-546.

33. Stabin MG, Sparks RB, Crowe E. OLINDA/EXM: the second-generation personal computer software for internal dose assessment in nuclear medicine. *J Nucl Med*. 2005;46:1023-1027.

34. Stabin MG. Uncertainties in internal dose calculations for radiopharmaceuticals. *j nucl med*. 2008;49:853-860.

35. Gear JI, Cox MG, Gustafsson J, et al. EANM practical guidance on uncertainty analysis for molecular radiotherapy absorbed dose calculations. *Eur J Nucl Med Mol Imaging*. 2018;45:2456-2474.

36. Zvereva A, Kamp F, Schlattl H, Zankl M, Parodi K. Impact of interpatient variability on organ dose estimates according to MIRD schema: Uncertainty and variance-based sensitivity analysis. *Med Phys*. 2018;45:3391-3403.

37. Weber W, Zanzonico P. The controversial linear no-threshold model. *J Nucl Med*. 2017;58:7-8.

38. Siegel JA, Pennington CW, Sacks B. Subjecting radiologic imaging to the linear no-threshold hypothesis: a non sequitur of non-trivial proportion. *J Nucl Med*. 2017;58:1-6.

39. Stabin MG, Emmons MA, Segars WP, Fernald MJ. Realistic reference adult and paediatric phantom series for internal and external dosimetry. *Radiat Prot Dosimetry*. 2012;149:56-59.

40. Menzel H-G, Clement C, DeLuca P. ICRP Publication 110. Realistic reference phantoms: an icrp/icru joint effort. a report of adult reference computational phantoms. *Ann ICRP*. 2009;39:1-164.

41. Andersson M, Johansson L, Eckerman K, Mattsson S. IDAC-Dose 2.1, an internal dosimetry program for diagnostic nuclear medicine based on the ICRP adult reference voxel phantoms. *EJNMMI Res*. 2017;7:88.

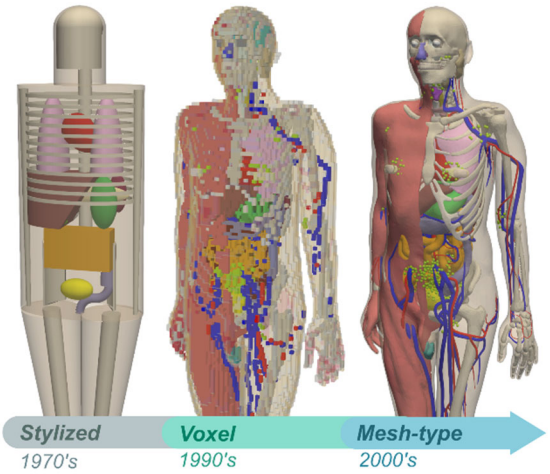

Figure 1: Comparison of phantom formats. *Left:* MIRD 5 era stylized adult anthropomorphic phantom (1969; ~25 source/target organs) used in OLINDA 1.0 and ICRP 128. *Middle:* ICRP 110 adult male voxel phantom (2009; 79 source regions, 43 target regions) used in IDAC-dose 2.1. *Right:* ICRP mesh reference adult male (2020; 190 source regions, 153 target regions) archetypal example used in this work.

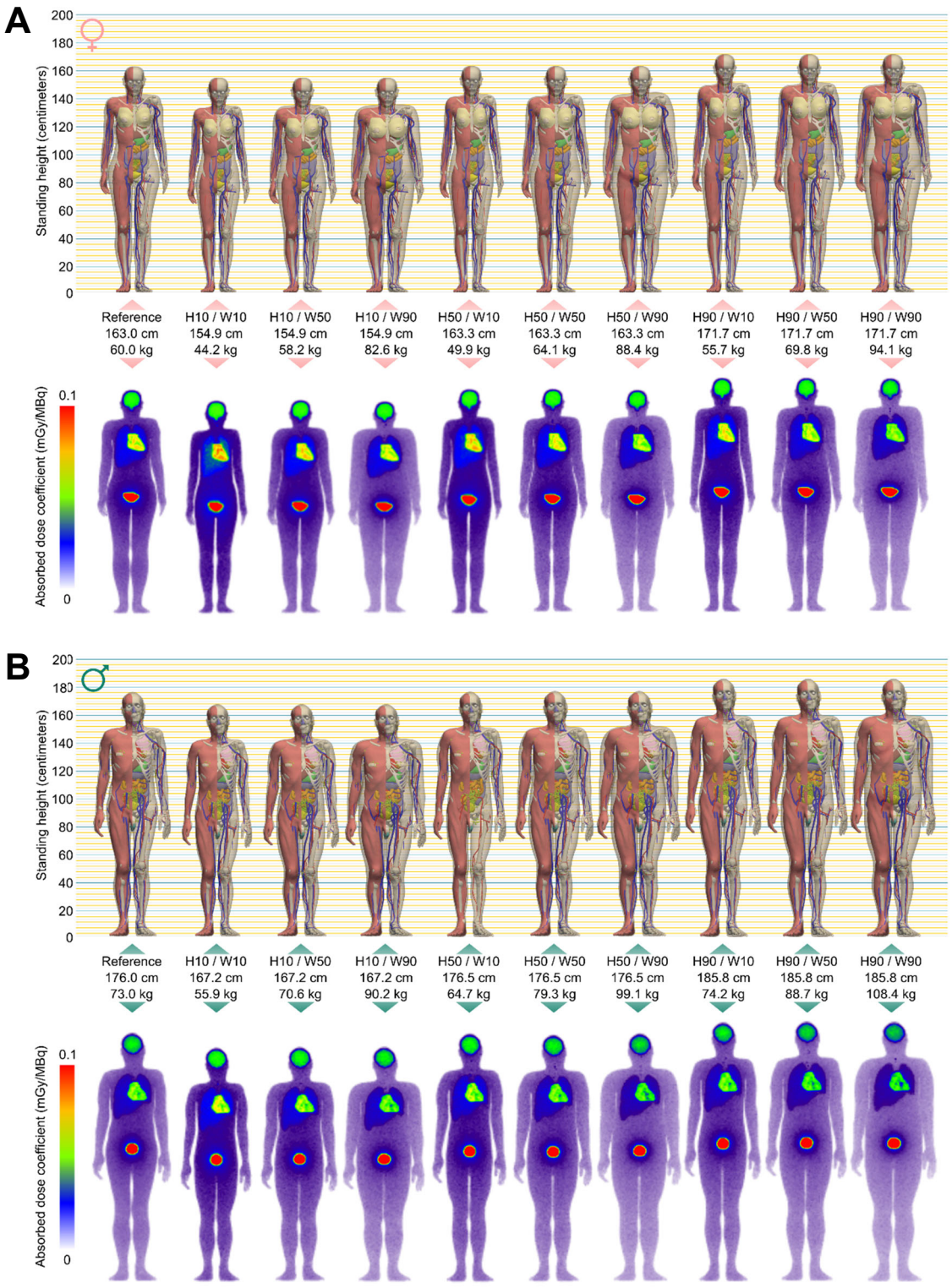

Figure 2: Voxel-level absorbed dose coefficients for ^{18}F-FDG. A) The adult female reference and percentile-specific phantom series juxtaposed with maximum intensity projections of their corresponding ^{18}F-FDG voxel dose coefficient maps. B) Same as (A) but for the adult male. Hx = x^{th} percentile standing height; Wy = y^{th} weight percentile within preceding standing height percentile.

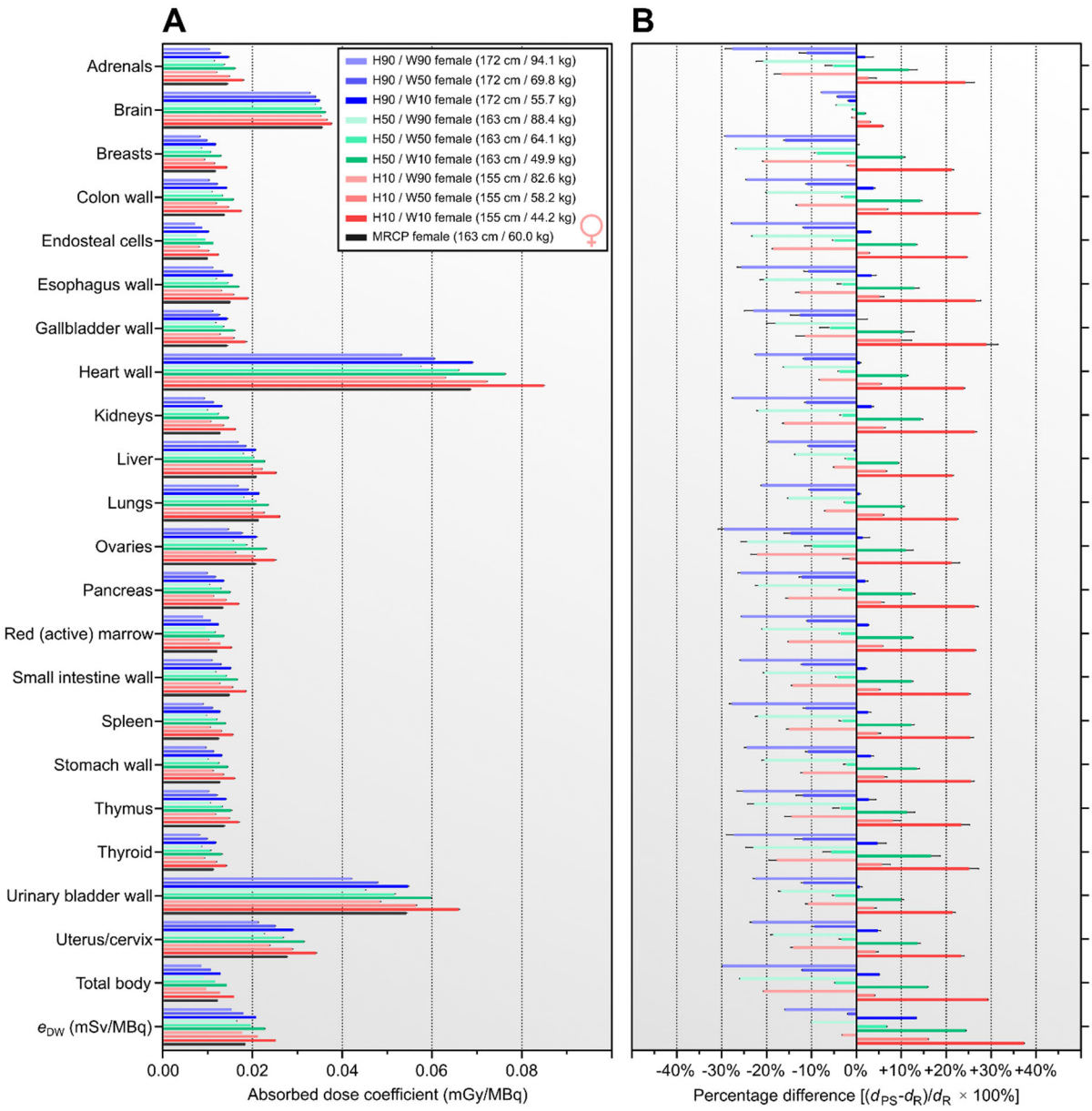

Figure 3: A) Organ-level absorbed dose coefficients for ^{18}F-FDG for the female mesh reference computational phantom (MRCP) and comparison with percentile-specific phantom series. B) Percentile specific dose coefficients presented as fractional differences relative to the reference female.

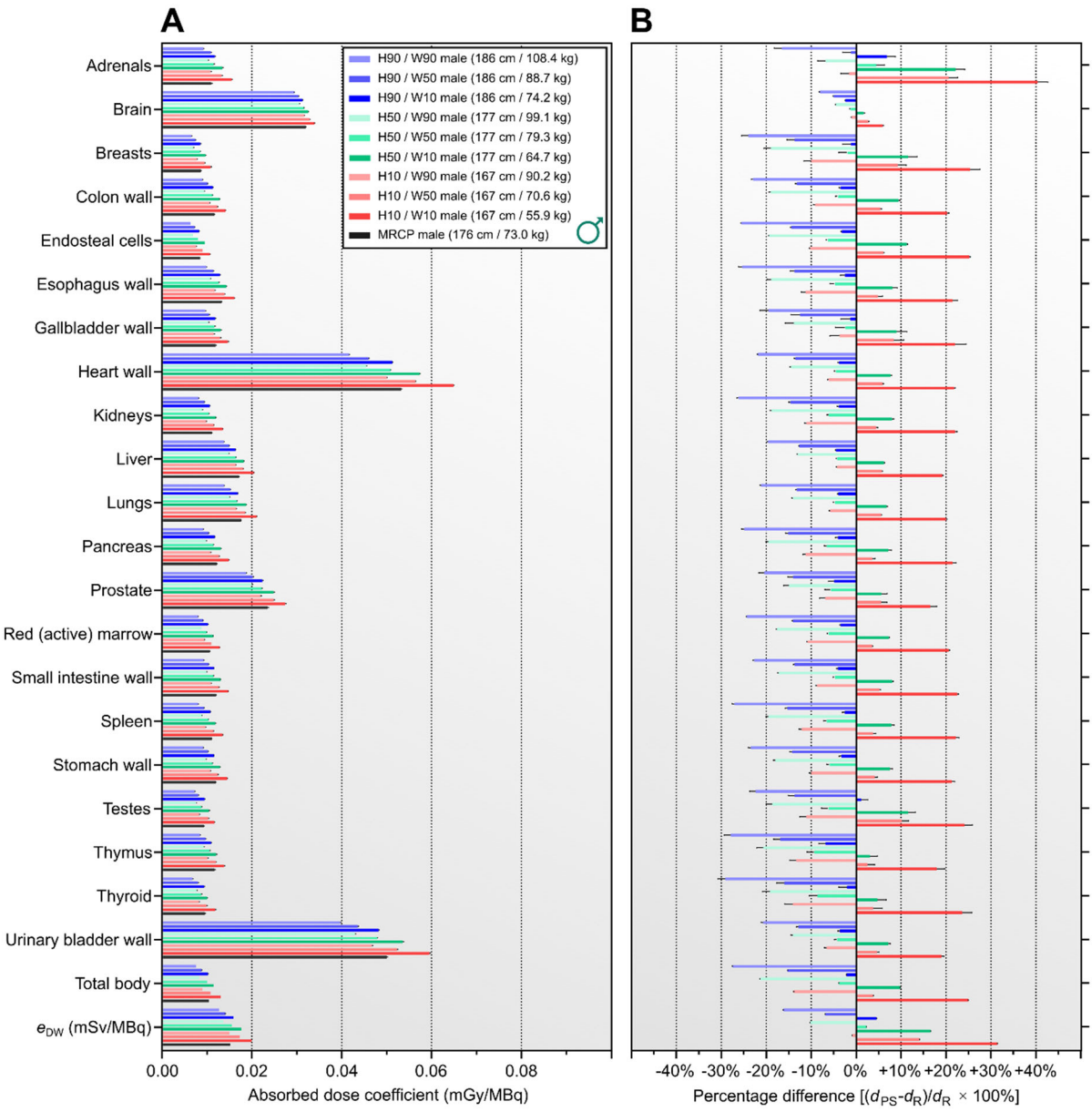

Figure 4: A) Organ-level absorbed dose coefficients for ^{18}F-FDG for the male mesh reference computational phantom and comparison with the percentile-specific phantom series. B) Percentile specific dose coefficients presented as fractional differences relative to the reference male.

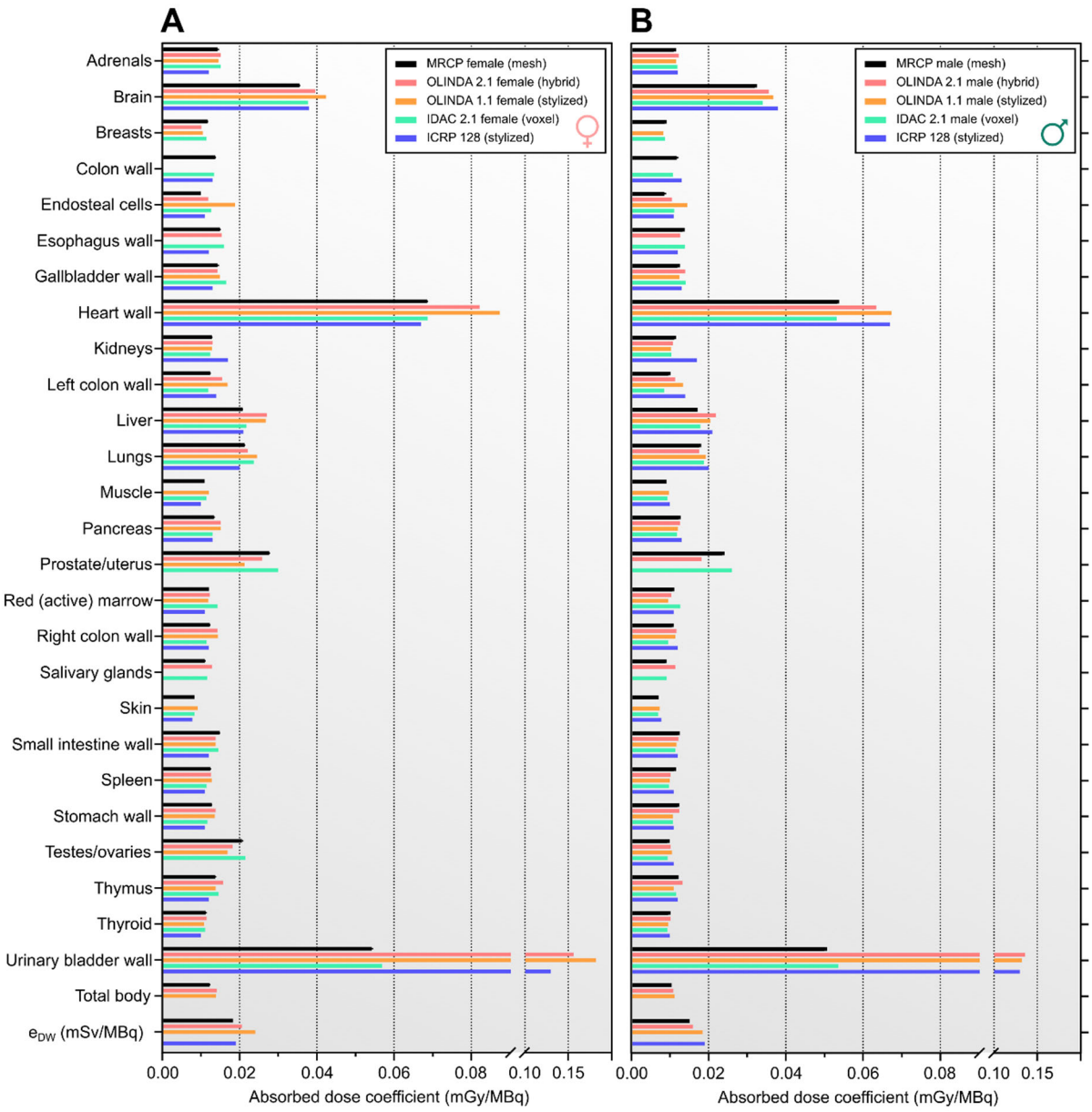

Figure 5: Comparison of organ-level dosimetry computed with reference phantoms in modern and legacy dosimetry software. Note the overall improved agreement between the mesh reference adults and the output of IDAC-dose 2.1, where anatomically equivalent phantoms were represented by different formats (i.e. mesh vs. voxel).

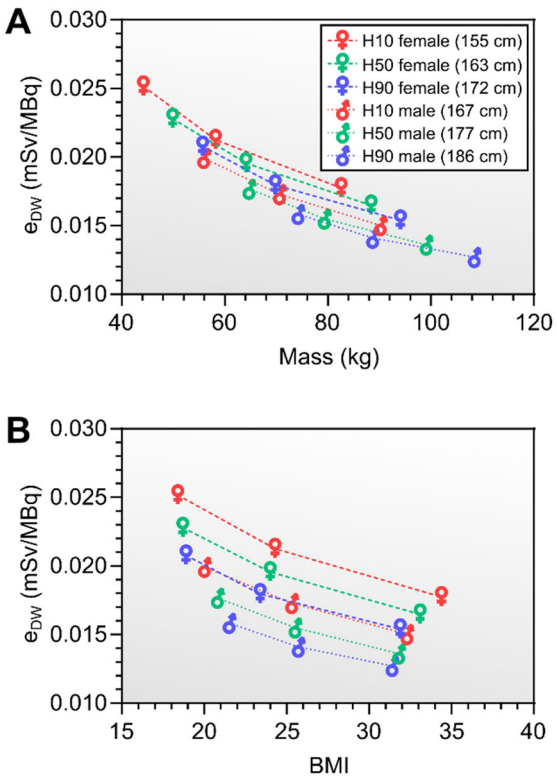

Figure 6: A) Dependence on body mass, and B) dependence on body mass index (BMI), of detriment-weighted dose coefficients for the male and female percentile specific phantom series.

Table 1: ICRP 128 reference organ time-integrated activity coefficients used in the present study.

Source organ/tissue	TIAC (h)
Brain	0.21
Heart wall	0.11
Lungs (alveolar interstitium)	0.079
Liver	0.13
Urinary bladder contents	0.26
Rest of body*	1.7

*Represents all other tissues – except for mineral bone, teeth, air within the body, and contents of the gastrointestinal tract – to which the associated TIAC is apportioned based on mass.

Table 2: Characteristics of phantoms as-implemented in software used in the present study.

Phantom name (software implementation)	**Morphometric category**	**Format**	**Source/target regions**	**Tissue weighting factors‡**	**Reference**
Mesh reference (PARaDIM)	Reference	Tetrahedral mesh	190	ICRP 103	(*20*)
Percentile-specific (PARaDIM)	Patient-dependent	Tetrahedral mesh	190	ICRP 103	(*22*)
ICRP 89 adult (OLINDA 2.1)	Reference	Hybrid*	27/25 (M) 28/26 (F)	ICRP 103	(*19*,*39*)
Cristy-Eckerman adult (OLINDA 1.1)	Reference	Stylized	26/25** (M) 25/24 (F)	ICRP 60	(*8*,*33*)
Cristy-Eckerman adult (ICRP 128)	Reference	Stylized	28†	ICRP 60	(*8*,*11*)
ICRP 110 adult (IDAC-dose 2.1)	Reference	Voxel	79/47	ICRP 103	(*40*,*41*)

*Hybrid non-uniform rational basis spline format converted to voxel format during calculations used in preparation for software implementation

†Hermaphroditic phantom containing male/female source/target organs

‡Tissue-specific weighting factors applied in computation of effective dose or detrimented-weighted dose coefficients

Graphical Abstract:

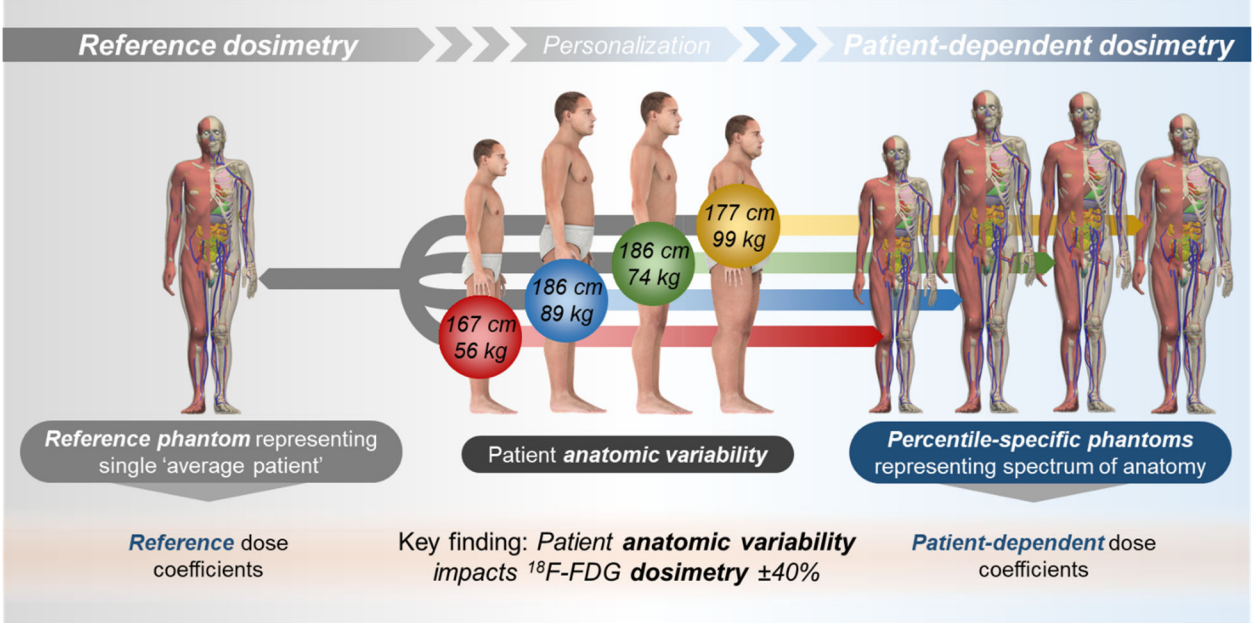

Supplementary Table S1: ^{18}F-FDG organ-level absorbed dose coefficients (mGy/MBq) for adult female reference phantoms.

Organ/tissue	Absorbed dose coefficient (mGy/MBq)			
	MRCP adult female (PARaDIM)	Adult female (IDAC-dose 2.1)	Adult female (OLINDA 1.1)	ICRP 89 adult female (OLINDA 2.1)
Red (active) marrow	0.01213 ± 0.000014	0.0143	0.0119	0.0123
Colon wall	0.013737 ± 0.000033	0.0134	--	--
Stem cells of colon	0.01302 ± 0.00023	--	--	--
Right lung + left lung	0.021312 ± 0.000032	0.0237	0.0245	0.0221
Stomach wall	0.012764 ± 0.000052	0.0117	0.0136	0.0138
Stem cells of stomach	0.01183 ± 0.00031	--	--	--
Breast adipose + breast glandular	0.011768 ± 0.000031	0.0114	0.0105	0.0101
Right ovary + left ovary	0.02062 ± 0.00023	0.0215	0.0169	0.0182
Testes	--	--	--	--
Urinary bladder wall	0.05426 ± 0.0002	0.0569	0.182	0.156
Urinary bladder basal cells	0.09012 ± 0.00088	--	--	--
Esophagus wall	0.01497 ± 0.00011	0.016	--	0.0154
Esophagus basal cells	0.01281 ± 0.00065	--	--	--
Liver	0.020802 ± 0.000027	0.0218	0.0268	0.0271
Thyroid	0.01126 ± 0.00015	0.0111	0.0108	0.0115
50um endosteal region (endosteal cells)	0.009982 ± 0.000012	0.0127	0.0189	0.0119
Brain	0.035548 ± 0.000043	0.0377	0.0424	0.0396
Salivary glands	0.011032 ± 0.000078	0.0116	--	0.0129
Skin	0.008345 ± 0.000011	0.00834	0.00911	--
Basal cells of skin	0.006693 ± 0.000027	--	--	--
Right adrenal + left adrenal	0.01437 ± 0.00018	0.0151	0.0146	0.0151
ET region	0.01163 ± 0.00014	0.00993	--	--
Gallbladder wall	0.01432 ± 0.00022	0.0165	0.0149	0.0143
Heart wall	0.06853 ± 0.00011	0.0687	0.0874	0.0821
Right kidney + left kidney	0.012808 ± 0.000038	0.0124	0.0129	0.013
Systemic lymph nodes	0.014099 ± 0.00006	0.0146	--	--

Muscle	0.010937 ± 0.0000057	0.0114	0.0121	--
Oral mucosa	0.01019 ± 0.00059	0.0112	--	--
Pancreas	0.013396 ± 0.000062	0.013	0.0151	0.0151
Prostate	--	--	--	--
Small intestine wall	0.014844 ± 0.000028	0.0145	0.0138	0.0138
Stem cells of small intestine	0.01358 ± 0.0002	--	--	--
Spleen	0.012479 ± 0.000054	0.0115	0.0128	0.0126
Thymus	0.0137 ± 0.00016	0.0146	0.0138	0.0158
Uterus/cervix	0.02771 ± 0.00011	0.03	0.0213	0.0259
Tongue	0.011183 ± 0.000086	0.00823	--	--
Tonsils	0.01218 ± 0.00037	0.0122	--	--
Right colon wall (ascending + right transverse)	0.012307 ± 0.00005	0.0115	0.0144	0.0143
Left colon wall (left transverse + descending)	0.012376 ± 0.00005	0.0119	0.0169	0.0155
Rectosigmoid colon wall (sigmoid + rectum)	0.019514 ± 0.000085	0.0202	--	--
Stem cells of right colon (ascending + right transverse)	0.01104 ± 0.00032	--	--	--
Stem cells of left colon (left transverse + descending)	0.01157 ± 0.00041	--	--	--
Stem cells of rectosigmoid colon (sigmoid + rectum)	0.01861 ± 0.00057	--	--	0.0256
Basal cells of anterior nasal passages	0.01 ± 0.0019	0.00727	--	--
Basal cells of posterior nasal passages + pharynx	0.01303 ± 0.00088	0.00993	--	--
Extrathoracic lymph nodes	0.01264 ± 0.00018	0.00766	--	--
Bronchial basal cells	0.0214 ± 0.0015	0.0206	--	--
Bronchial secretory cells	0.0213 ± 0.0015	0.0206	--	--
Bronchiolar secretory cells	--	0.0252	--	--
Alveolar-interstitium	0.021312 ± 0.000032	0.0252	--	--
Thoracic lymph nodes	0.01375 ± 0.00019	0.0127	--	--
Right lung lobe	0.021223 ± 0.000042	--	--	--
Left lung lobe	0.02142 ± 0.000047	--	--	--
Right adrenal gland	0.01433 ± 0.00024	--	--	--

Left adrenal gland	0.01441 ± 0.00027	--	--	--
Right breast adipose	0.010936 ± 0.000054	--	--	--
Right breast glandular	0.011192 ± 0.000069	--	--	--
Left breast adipose	0.011576 ± 0.000056	--	--	--
Left breast glandular	0.012056 ± 0.000071	--	--	--
Right breast (adipose + glandular)	0.011039 ± 0.000042	--	--	--
Left breast (adipose + glandular)	0.011768 ± 0.000044	--	--	--
Breast (adipose)	0.011576 ± 0.000039	--	--	--
Breast (glandular)	0.012056 ± 0.00005	--	--	--
Entire lenses of eye	0.01094 ± 0.00088	0.00926	--	0.0129
Sensitive lenses of eye	0.0131 ± 0.0021	--	--	--
Right kidney cortex	0.013276 ± 0.000065	--	--	--
Right kidney medulla	0.01315 ± 0.00012	--	--	--
Right kidney pelvis	0.01371 ± 0.00027	--	--	--
Right kidney (cortex + medulla + pelvis)	0.013268 ± 0.000056	--	--	--
Left kidney cortex	0.01241 ± 0.000058	--	--	--
Left kidney medulla	0.01248 ± 0.00011	--	--	--
Left kidney pelvis	0.01235 ± 0.00024	--	--	--
Left kidney (cortex + medulla + pelvis)	0.012421 ± 0.000051	--	--	--
Right ovary	0.02006 ± 0.00032	--	--	--
Left ovary	0.02062 ± 0.00033	--	--	--
Pituitary gland	0.0215 ± 0.0011	0.0217	--	--
Spinal cord	0.01271 ± 0.00015	--	--	--
Ureters	0.0153 ± 0.00018	0.0166	--	--
Adipose/residual tissue	0.0104791 ± 0.0000047	0.0107	--	--
Total body	0.0122857 ± 0.0000033	--	0.0139	0.0141
e_{DW} or e (mSv/MBq)	0.0183177 ± 0.0000033	0.0161	0.0241	0.0206

Supplementary Table S2: ^{18}F-FDG organ-level absorbed dose coefficients (mGy/MBq) for adult male reference phantoms.

Organ/tissue	Absorbed dose coefficient (mGy/MBq)			
	MRCP adult male (PARaDIM)	Adult male (IDAC-dose 2.1)	Adult male (OLINDA 1.1)	ICRP 89 adult male (OLINDA 2.1)
Red (active) marrow	0.010647 ± 0.000012	0.0127	0.00959	0.0104
Colon wall	0.01174 ± 0.000029	0.0107	--	--
Stem cells of colon	0.01085 ± 0.00021	--	--	--
Right lung + left lung	0.01759 ± 0.000026	0.0188	0.0193	0.0176
Stomach wall	0.011973 ± 0.000046	0.0107	0.0107	0.0124
Stem cells of stomach	0.01016 ± 0.00026	--	--	--
Breast adipose + breast glandular	0.00865 ± 0.00011	0.00874	0.00827	--
Right ovary + left ovary	--	--	0.0135	--
Testes	0.009375 ± 0.000098	0.00943	0.0105	0.0102
Urinary bladder wall	0.05002 ± 0.00017	0.0536	0.132	0.136
Urinary bladder basal cells	0.08941 ± 0.00091	--	--	--
Esophagus wall	0.013262 ± 0.000092	0.0138	--	0.0127
Esophagus basal cells	0.01274 ± 0.00063	--	--	--
Liver	0.017163 ± 0.000021	0.0179	0.0205	0.0219
Thyroid	0.00958 ± 0.00013	0.00935	0.0096	0.0101
50um endosteal region (endosteal cells)	0.0085496 ± 0.0000095	0.0111	0.0145	0.0105
Brain	0.032021 ± 0.000038	0.034	0.0368	0.0356
Salivary glands	0.00868 ± 0.000063	0.00916	--	0.0114
Skin	0.0070636 ± 0.0000083	0.007	0.00736	--
Basal cells of skin	0.005614 ± 0.000023	--	--	--
Right adrenal + left adrenal	0.01102 ± 0.00015	0.0119	0.0116	0.0123
ET region	0.009422 ± 0.00009	0.00858	--	--
Gallbladder wall	0.01196 ± 0.00018	0.0141	0.0125	0.014
Heart wall	0.053279 ± 0.000085	0.0532	0.0674	0.0634
Right kidney + left kidney	0.011098 ± 0.000032	0.0104	0.0103	0.0107
Systemic lymph nodes	0.012935 ± 0.000052	0.0133	--	--

Muscle	0.0090788 ± 0.0000037	0.00939	0.00974	--
Oral mucosa	0.00888 ± 0.00047	0.00973	--	--
Pancreas	0.012247 ± 0.000054	0.0118	0.0121	0.0126
Prostate	0.02352 ± 0.00021	0.0261	--	0.0182
Small intestine wall	0.012067 ± 0.000022	0.0114	0.0117	0.0122
Stem cells of small intestine	0.01109 ± 0.00016	--	--	--
Spleen	0.011052 ± 0.000045	0.00979	0.01	0.0101
Thymus	0.01171 ± 0.00013	0.0116	0.011	0.0133
Uterus/cervix	--	--	0.0179	--
Tongue	0.00931 ± 0.00007	0.00751	--	--
Tonsils	0.01217 ± 0.00037	0.0127	--	--
Right colon wall (ascending + right transverse)	0.010522 ± 0.000043	0.00955	0.0114	0.0117
Left colon wall (left transverse + descending)	0.009657 ± 0.000042	0.00854	0.0134	0.0113
Rectosigmoid colon wall (sigmoid + rectum)	0.017655 ± 0.000078	0.0175	--	--
Stem cells of right colon (ascending + right transverse)	0.00988 ± 0.00032	--	--	--
Stem cells of left colon (left transverse + descending)	0.00911 ± 0.00034	--	--	--
Stem cells of rectosigmoid colon (sigmoid + rectum)	0.01457 ± 0.00048	--	--	0.0157
Basal cells of anterior nasal passages	0.0087 ± 0.0011	0.00524	--	--
Basal cells of posterior nasal passages + pharynx	0.01061 ± 0.00065	0.00858	--	--
Extrathoracic lymph nodes	0.01058 ± 0.00015	0.00585	--	--
Bronchial basal cells	0.01575 ± 0.00084	0.015	--	--
Bronchial secretory cells	0.01569 ± 0.00084	0.015	--	--
Bronchiolar secretory cells	--	0.0207	--	--
Alveolar-interstitium	0.01759 ± 0.000026	0.0206	--	--
Thoracic lymph nodes	0.01222 ± 0.00016	0.0108	--	--
Right lung lobe	0.017566 ± 0.000035	--	--	--
Left lung lobe	0.017619 ± 0.000039	--	--	--
Right adrenal gland	0.01204 ± 0.00022	--	--	--

Left adrenal gland	0.01102 ± 0.00021	--	--	--
Right breast adipose	0.00909 ± 0.00021	--	--	--
Right breast glandular	0.00788 ± 0.00023	--	--	--
Left breast adipose	0.00903 ± 0.00021	--	--	--
Left breast glandular	0.00808 ± 0.00024	--	--	--
Right breast (adipose + glandular)	0.0086 ± 0.00016	--	--	--
Left breast (adipose + glandular)	0.00865 ± 0.00016	--	--	--
Breast (adipose)	0.00903 ± 0.00015	--	--	--
Breast (glandular)	0.00808 ± 0.00017	--	--	--
Entire lenses of eye	0.00927 ± 0.00082	0.00811	--	0.0103
Sensitive lenses of eye	0.0064 ± 0.0015	--	--	--
Right kidney cortex	0.011438 ± 0.000053	--	--	--
Right kidney medulla	0.01168 ± 0.0001	--	--	--
Right kidney pelvis	0.01224 ± 0.00023	--	--	--
Right kidney (cortex + medulla + pelvis)	0.011512 ± 0.000046	--	--	--
Left kidney cortex	0.010648 ± 0.000051	--	--	--
Left kidney medulla	0.01073 ± 0.0001	--	--	--
Left kidney pelvis	0.01088 ± 0.00022	--	--	--
Left kidney (cortex + medulla + pelvis)	0.010672 ± 0.000045	--	--	--
Right ovary	--	--	--	--
Left ovary	--	--	--	--
Pituitary gland	0.01833 ± 0.00098	0.0197	--	--
Spinal cord	0.010817 ± 0.0001	--	--	--
Ureters	0.01463 ± 0.00017	0.0146	--	--
Adipose/residual tissue	0.0093647 ± 0.0000047	0.0096	--	--
Total body	0.0104552 ± 0.0000027	--	0.0112	0.0109
e_{DW} or e (mSv/MBq)	0.0151539 ± 0.0000033	0.0161	0.0185	0.016

Supplementary Table S3: ^{18}F-FDG organ-level absorbed dose coefficients (mGy/MBq) for the 10th percentile standing height adult female PSPs.

Organ/tissue	Absorbed dose coefficient (mGy/MBq)		
	H10 / W10 female (155 cm / 44.2 kg)	H10 / W50 female (155 cm / 58.2 kg)	H10 / W90 female (155 cm / 82.6 kg)
Red (active) marrow	0.015334 ± 0.000018	0.012833 ± 0.000015	0.010297 ± 0.000012
Colon wall	0.017473 ± 0.000042	0.014658 ± 0.000035	0.011937 ± 0.000028
Stem cells of colon	0.01653 ± 0.00029	0.01435 ± 0.00025	0.01167 ± 0.00022
Right lung + left lung	0.026091 ± 0.00004	0.022572 ± 0.000033	0.019841 ± 0.000029
Stomach wall	0.016024 ± 0.000065	0.013563 ± 0.000055	0.011242 ± 0.000045
Stem cells of stomach	0.01398 ± 0.00037	0.0119 ± 0.00031	0.01012 ± 0.00026
Breast adipose + breast glandular	0.014271 ± 0.000041	0.011565 ± 0.000031	0.009342 ± 0.000022
Right ovary + left ovary	0.02499 ± 0.00029	0.02031 ± 0.00024	0.01608 ± 0.00019
Testes	--	--	--
Urinary bladder wall	0.06589 ± 0.00024	0.05637 ± 0.0002	0.04839 ± 0.00018
Urinary bladder basal cells	0.11854 ± 0.001	0.10008 ± 0.00085	0.08589 ± 0.00074
Esophagus wall	0.01894 ± 0.00014	0.01574 ± 0.00011	0.013079 ± 0.000094
Esophagus basal cells	0.01782 ± 0.00086	0.0154 ± 0.00075	0.01266 ± 0.00064
Liver	0.025256 ± 0.000033	0.022164 ± 0.000029	0.019771 ± 0.000024
Thyroid	0.01408 ± 0.00019	0.01189 ± 0.00016	0.00926 ± 0.00013
50um endosteal region (endosteal cells)	0.012432 ± 0.000015	0.010259 ± 0.000013	0.008124 ± 0.00001
Brain	0.037615 ± 0.000045	0.036608 ± 0.000044	0.035228 ± 0.000042
Salivary glands	0.013904 ± 0.000096	0.011245 ± 0.00008	0.008813 ± 0.000067
Skin	0.011073 ± 0.000014	0.008728 ± 0.000011	0.006281 ± 0.0000084
Basal cells of skin	0.008799 ± 0.000034	0.006952 ± 0.000029	0.005219 ± 0.000022
Right adrenal + left adrenal	0.01784 ± 0.00023	0.01475 ± 0.00019	0.01197 ± 0.00015
ET region	0.01445 ± 0.00017	0.01181 ± 0.00015	0.00927 ± 0.00012
Gallbladder wall	0.01846 ± 0.00029	0.01575 ± 0.00024	0.01268 ± 0.0002
Heart wall	0.0849 ± 0.00014	0.07222 ± 0.00012	0.06295 ± 0.0001
Right kidney + left kidney	0.016184 ± 0.000047	0.013585 ± 0.000039	0.010749 ± 0.000031
Systemic lymph nodes	0.01784 ± 0.000074	0.014961 ± 0.000061	0.012048 ± 0.000049

Muscle	0.013979 ± 0.0000056	0.011284 ± 0.0000056	0.0086685 ± 0.0000043
Oral mucosa	0.01264 ± 0.0007	0.00997 ± 0.00058	0.00769 ± 0.00051
Pancreas	0.016924 ± 0.000078	0.014136 ± 0.000065	0.011366 ± 0.000051
Prostate	--	--	--
Small intestine wall	0.018565 ± 0.000035	0.015591 ± 0.000029	0.012732 ± 0.000024
Stem cells of small intestine	0.01702 ± 0.00024	0.01417 ± 0.00021	0.01193 ± 0.00018
Spleen	0.015641 ± 0.000069	0.013071 ± 0.000056	0.010608 ± 0.000046
Thymus	0.01691 ± 0.0002	0.01481 ± 0.00017	0.01172 ± 0.00013
Uterus/cervix	0.03418 ± 0.00014	0.0289 ± 0.00012	0.023798 ± 0.000095
Tongue	0.01415 ± 0.00011	0.011383 ± 0.000089	0.008811 ± 0.000072
Tonsils	0.01554 ± 0.00046	0.01158 ± 0.00037	0.00973 ± 0.00032
Right colon wall (ascending + right transverse)	0.015622 ± 0.000063	0.013245 ± 0.000052	0.010818 ± 0.000043
Left colon wall (left transverse + descending)	0.015855 ± 0.000065	0.013315 ± 0.000054	0.010855 ± 0.000043
Rectosigmoid colon wall (sigmoid + rectum)	0.02449 ± 0.00013	0.02018 ± 0.00011	0.016496 ± 0.000089
Stem cells of right colon (ascending + right transverse)	0.01434 ± 0.0004	0.01237 ± 0.00034	0.00984 ± 0.00029
Stem cells of left colon (left transverse + descending)	0.01458 ± 0.0005	0.0124 ± 0.00042	0.01078 ± 0.00037
Stem cells of rectosigmoid colon (sigmoid + rectum)	0.02316 ± 0.0007	0.0206 ± 0.00064	0.0163 ± 0.00053
Basal cells of anterior nasal passages	0.0131 ± 0.0028	0.0112 ± 0.002	0.0066 ± 0.0016
Basal cells of posterior nasal passages + pharynx	0.025 ± 0.0026	0.0187 ± 0.0021	0.0152 ± 0.0017
Extrathoracic lymph nodes	0.01589 ± 0.00022	0.01344 ± 0.00019	0.01058 ± 0.00016
Bronchial basal cells	0.0247 ± 0.0017	0.0187 ± 0.0014	0.0166 ± 0.0013
Bronchial secretory cells	0.024 ± 0.0018	0.0202 ± 0.0015	0.0166 ± 0.0014
Bronchiolar secretory cells	--	--	--
Alveolar-interstitium	0.026091 ± 0.00004	0.022572 ± 0.000033	0.019841 ± 0.000029
Thoracic lymph nodes	0.01722 ± 0.00024	0.01488 ± 0.0002	0.01148 ± 0.00016
Right lung lobe	0.025962 ± 0.000055	0.022524 ± 0.000045	0.019797 ± 0.00004
Left lung lobe	0.026249 ± 0.000058	0.022631 ± 0.00005	0.019895 ± 0.000044
Right adrenal gland	0.01785 ± 0.00031	0.01482 ± 0.00025	0.01192 ± 0.0002

Left adrenal gland	0.01783 ± 0.00034	0.01465 ± 0.00028	0.01203 ± 0.00023
Right breast adipose	0.014238 ± 0.000077	0.011474 ± 0.000055	0.009286 ± 0.000036
Right breast glandular	0.014311 ± 0.000087	0.011711 ± 0.000073	0.009482 ± 0.000058
Left breast adipose	0.014691 ± 0.000078	0.011993 ± 0.000056	0.009793 ± 0.000037
Left breast glandular	0.015602 ± 0.00009	0.01262 ± 0.000074	0.010257 ± 0.000061
Right breast (adipose + glandular)	0.014271 ± 0.000058	0.011565 ± 0.000044	0.009342 ± 0.000031
Left breast (adipose + glandular)	0.015107 ± 0.000059	0.012233 ± 0.000045	0.009925 ± 0.000032
Breast (adipose)	0.014238 ± 0.000054	0.011474 ± 0.000039	0.009286 ± 0.000026
Breast (glandular)	0.014311 ± 0.000062	0.011711 ± 0.000051	0.009482 ± 0.000041
Entire lenses of eye	0.0127 ± 0.001	0.0121 ± 0.001	0.00635 ± 0.00064
Sensitive lenses of eye	0.0101 ± 0.002	0.0113 ± 0.002	0.0072 ± 0.0015
Right kidney cortex	0.016678 ± 0.000082	0.013987 ± 0.000069	0.011172 ± 0.000055
Right kidney medulla	0.01676 ± 0.00016	0.01413 ± 0.00013	0.01126 ± 0.00011
Right kidney pelvis	0.0168 ± 0.00035	0.0142 ± 0.00028	0.01125 ± 0.00023
Right kidney (cortex + medulla + pelvis)	0.016698 ± 0.000071	0.014022 ± 0.000059	0.011192 ± 0.000048
Left kidney cortex	0.015602 ± 0.000073	0.013165 ± 0.000062	0.010312 ± 0.000049
Left kidney medulla	0.01551 ± 0.00014	0.01296 ± 0.00012	0.010182 ± 0.000092
Left kidney pelvis	0.01623 ± 0.00031	0.01289 ± 0.00025	0.01029 ± 0.0002
Left kidney (cortex + medulla + pelvis)	0.015608 ± 0.000064	0.013114 ± 0.000053	0.010286 ± 0.000043
Right ovary	0.02499 ± 0.00041	0.02031 ± 0.00033	0.01608 ± 0.00027
Left ovary	0.0255 ± 0.00041	0.02167 ± 0.00034	0.01676 ± 0.00027
Pituitary gland	0.0228 ± 0.0012	0.0225 ± 0.0011	0.01731 ± 0.00089
Spinal cord	0.01572 ± 0.00019	0.01299 ± 0.00016	0.01042 ± 0.00013
Ureters	0.01981 ± 0.00023	0.01624 ± 0.00018	0.01304 ± 0.00015
Adipose/residual tissue	0.013802 ± 0.0000055	0.010997 ± 0.0000044	0.0083336 ± 0.0000025
Total body	0.0158901 ± 0.0000039	0.0127871 ± 0.0000033	0.0097375 ± 0.0000022
e_{DW} or e (mSv/MBq)	0.0251598 ± 0.0000049	0.0212562 ± 0.0000035	0.0177345 ± 0.0000026

Supplementary Table S4: ^{18}F-FDG organ-level absorbed dose coefficients (mGy/MBq) for the 50th percentile standing height adult female PSPs.

Organ/tissue	Absorbed dose coefficient (mGy/MBq)		
	H50 / W10 female (163 cm / 49.9 kg)	H50 / W50 female (163 cm / 64.1 kg)	H50 / W90 female (163 cm / 88.4 kg)
Red (active) marrow	0.013634 ± 0.000016	0.011682 ± 0.000014	0.009585 ± 0.000011
Colon wall	0.015696 ± 0.000038	0.013327 ± 0.000032	0.011004 ± 0.000026
Stem cells of colon	0.0147 ± 0.00026	0.01309 ± 0.00024	0.01083 ± 0.0002
Right lung + left lung	0.023533 ± 0.000036	0.020768 ± 0.000031	0.018083 ± 0.000027
Stomach wall	0.014479 ± 0.000059	0.012473 ± 0.000049	0.010142 ± 0.000041
Stem cells of stomach	0.0128 ± 0.00034	0.01154 ± 0.0003	0.00932 ± 0.00025
Breast adipose + breast glandular	0.012993 ± 0.000037	0.010703 ± 0.000028	0.008636 ± 0.000021
Right ovary + left ovary	0.02287 ± 0.00026	0.01856 ± 0.00021	0.01561 ± 0.00018
Testes	--	--	--
Urinary bladder wall	0.05968 ± 0.00022	0.05163 ± 0.00019	0.04511 ± 0.00016
Urinary bladder basal cells	0.10669 ± 0.00091	0.09122 ± 0.00078	0.07834 ± 0.00067
Esophagus wall	0.0169 ± 0.00012	0.01448 ± 0.0001	0.011888 ± 0.000085
Esophagus basal cells	0.01591 ± 0.00077	0.01396 ± 0.0007	0.01156 ± 0.0006
Liver	0.022741 ± 0.00003	0.020317 ± 0.000024	0.017978 ± 0.000022
Thyroid	0.01313 ± 0.00017	0.01062 ± 0.00014	0.00867 ± 0.00012
50um endosteal region (endosteal cells)	0.011315 ± 0.000014	0.009466 ± 0.000012	0.0076684 ± 0.0000097
Brain	0.036225 ± 0.000043	0.035266 ± 0.000042	0.033984 ± 0.000041
Salivary glands	0.012855 ± 0.000089	0.010565 ± 0.000076	0.00835 ± 0.000063
Skin	0.009779 ± 0.000012	0.0079561 ± 0.0000099	0.0058909 ± 0.0000079
Basal cells of skin	0.007869 ± 0.000031	0.006379 ± 0.000026	0.00489 ± 0.000021
Right adrenal + left adrenal	0.01604 ± 0.0002	0.01361 ± 0.00017	0.01138 ± 0.00014
ET region	0.01306 ± 0.00016	0.01098 ± 0.00014	0.00881 ± 0.00012
Gallbladder wall	0.01583 ± 0.00025	0.01346 ± 0.00021	0.01173 ± 0.00018
Heart wall	0.07625 ± 0.00012	0.06587 ± 0.00011	0.05745 ± 0.000092
Right kidney + left kidney	0.014645 ± 0.000043	0.012384 ± 0.000035	0.010012 ± 0.000029
Systemic lymph nodes	0.016022 ± 0.000066	0.013618 ± 0.000055	0.011164 ± 0.000045

Muscle	0.012582 ± 0.000005	0.010326 ± 0.0000052	0.0081449 ± 0.0000041
Oral mucosa	0.01257 ± 0.00071	0.01084 ± 0.0006	0.00784 ± 0.0005
Pancreas	0.015052 ± 0.000069	0.01295 ± 0.000058	0.010458 ± 0.000048
Prostate	--	--	--
Small intestine wall	0.01667 ± 0.000031	0.014188 ± 0.000026	0.011796 ± 0.000022
Stem cells of small intestine	0.01571 ± 0.00022	0.01322 ± 0.00019	0.01096 ± 0.00016
Spleen	0.014005 ± 0.00006	0.012071 ± 0.000051	0.009742 ± 0.000042
Thymus	0.01524 ± 0.00018	0.01319 ± 0.00015	0.01058 ± 0.00012
Uterus/cervix	0.03147 ± 0.00012	0.02679 ± 0.0001	0.022556 ± 0.000088
Tongue	0.012787 ± 0.000097	0.010506 ± 0.000083	0.008342 ± 0.000069
Tonsils	0.01354 ± 0.00041	0.01092 ± 0.00035	0.00932 ± 0.00031
Right colon wall (ascending + right transverse)	0.013923 ± 0.000056	0.011985 ± 0.000047	0.010004 ± 0.000039
Left colon wall (left transverse + descending)	0.014236 ± 0.000058	0.012005 ± 0.000049	0.009857 ± 0.00004
Rectosigmoid colon wall (sigmoid + rectum)	0.02215 ± 0.00012	0.0187 ± 0.000099	0.015476 ± 0.000082
Stem cells of right colon (ascending + right transverse)	0.01273 ± 0.00036	0.01109 ± 0.00031	0.00925 ± 0.00027
Stem cells of left colon (left transverse + descending)	0.0125 ± 0.00043	0.01185 ± 0.00041	0.00962 ± 0.00035
Stem cells of rectosigmoid colon (sigmoid + rectum)	0.02119 ± 0.00064	0.01847 ± 0.00059	0.01538 ± 0.00048
Basal cells of anterior nasal passages	0.0149 ± 0.0023	0.0076 ± 0.0014	0.0067 ± 0.0013
Basal cells of posterior nasal passages + pharynx	0.0244 ± 0.0025	0.0173 ± 0.002	0.0145 ± 0.0015
Extrathoracic lymph nodes	0.01432 ± 0.0002	0.01198 ± 0.00018	0.00997 ± 0.00015
Bronchial basal cells	0.0227 ± 0.0016	0.0182 ± 0.0014	0.0151 ± 0.0011
Bronchial secretory cells	0.0242 ± 0.0017	0.017 ± 0.0013	0.0158 ± 0.0012
Bronchiolar secretory cells	--	--	--
Alveolar-interstitium	0.023533 ± 0.000036	0.020768 ± 0.000031	0.018083 ± 0.000027
Thoracic lymph nodes	0.01539 ± 0.00021	0.01346 ± 0.00018	0.01061 ± 0.00015
Right lung lobe	0.023444 ± 0.000049	0.020682 ± 0.000041	0.01803 ± 0.000036
Left lung lobe	0.023641 ± 0.000052	0.020872 ± 0.000046	0.018147 ± 0.00004
Right adrenal gland	0.01601 ± 0.00027	0.01358 ± 0.00023	0.01158 ± 0.00019

Left adrenal gland	0.01608 ± 0.00031	0.01365 ± 0.00026	0.01113 ± 0.00021
Right breast adipose	0.012862 ± 0.000068	0.010552 ± 0.00005	0.008584 ± 0.000034
Right breast glandular	0.013153 ± 0.000079	0.010946 ± 0.000067	0.008761 ± 0.000054
Left breast adipose	0.013579 ± 0.000071	0.011169 ± 0.000051	0.008955 ± 0.000035
Left breast glandular	0.014177 ± 0.000081	0.011682 ± 0.000068	0.009502 ± 0.000055
Right breast (adipose + glandular)	0.012993 ± 0.000052	0.010703 ± 0.00004	0.008636 ± 0.000029
Left breast (adipose + glandular)	0.013847 ± 0.000053	0.011366 ± 0.000041	0.009116 ± 0.00003
Breast (adipose)	0.012862 ± 0.000048	0.010552 ± 0.000035	0.008584 ± 0.000024
Breast (glandular)	0.013153 ± 0.000056	0.010946 ± 0.000047	0.008761 ± 0.000038
Entire lenses of eye	0.01242 ± 0.00099	0.01038 ± 0.00089	0.00762 ± 0.00067
Sensitive lenses of eye	0.0116 ± 0.0019	0.0111 ± 0.0021	0.0075 ± 0.0014
Right kidney cortex	0.015006 ± 0.000075	0.012723 ± 0.000062	0.010385 ± 0.000051
Right kidney medulla	0.01485 ± 0.00014	0.01255 ± 0.00012	0.010395 ± 0.000096
Right kidney pelvis	0.01523 ± 0.0003	0.0134 ± 0.00026	0.01077 ± 0.00021
Right kidney (cortex + medulla + pelvis)	0.014985 ± 0.000065	0.012716 ± 0.000054	0.010402 ± 0.000044
Left kidney cortex	0.014221 ± 0.000067	0.011996 ± 0.000055	0.00958 ± 0.000045
Left kidney medulla	0.01431 ± 0.00013	0.01205 ± 0.00011	0.009548 ± 0.000086
Left kidney pelvis	0.01484 ± 0.00028	0.01215 ± 0.00023	0.00964 ± 0.00019
Left kidney (cortex + medulla + pelvis)	0.014262 ± 0.000058	0.012012 ± 0.000048	0.009576 ± 0.000039
Right ovary	0.02287 ± 0.00037	0.01856 ± 0.0003	0.01561 ± 0.00025
Left ovary	0.02401 ± 0.00038	0.01985 ± 0.00031	0.01611 ± 0.00025
Pituitary gland	0.0206 ± 0.0011	0.01846 ± 0.00096	0.01562 ± 0.00085
Spinal cord	0.01433 ± 0.00017	0.01215 ± 0.00014	0.00956 ± 0.00012
Ureters	0.01715 ± 0.0002	0.01472 ± 0.00017	0.01276 ± 0.00014
Adipose/residual tissue	0.012349 ± 0.0000049	0.010023 ± 0.000004	0.0077491 ± 0.0000023
Total body	0.0142377 ± 0.0000035	0.0116895 ± 0.000003	0.0090949 ± 0.0000021
e_{DW} or e (mSv/MBq)	0.0227877 ± 0.000004	0.0195576 ± 0.000003	0.0164682 ± 0.0000022

Supplementary Table S5: ^{18}F-FDG organ-level absorbed dose coefficients (mGy/MBq) for the 90th percentile standing height adult female PSPs.

Organ/tissue	Absorbed dose coefficient (mGy/MBq)		
	H90 / W10 female (172 cm / 55.7 kg)	H90 / W50 female (172 cm / 69.8 kg)	H90 / W90 female (172 cm / 94.1 kg)
Red (active) marrow	0.012448 ± 0.000015	0.010804 ± 0.000013	0.009027 ± 0.000011
Colon wall	0.014262 ± 0.000034	0.01223 ± 0.000029	0.010389 ± 0.000024
Stem cells of colon	0.01414 ± 0.00025	0.0113 ± 0.00021	0.0104 ± 0.00019
Right lung + left lung	0.021473 ± 0.000032	0.019091 ± 0.000028	0.016812 ± 0.000025
Stomach wall	0.013184 ± 0.000054	0.011382 ± 0.000045	0.009647 ± 0.000038
Stem cells of stomach	0.01151 ± 0.0003	0.01026 ± 0.00027	0.00833 ± 0.00022
Breast adipose + breast glandular	0.011798 ± 0.000033	0.009898 ± 0.000026	0.008348 ± 0.00002
Right ovary + left ovary	0.0209 ± 0.00023	0.0176 ± 0.0002	0.01455 ± 0.00016
Testes	--	--	--
Urinary bladder wall	0.05467 ± 0.0002	0.04784 ± 0.00017	0.04204 ± 0.00015
Urinary bladder basal cells	0.09665 ± 0.00082	0.08404 ± 0.00072	0.07277 ± 0.00063
Esophagus wall	0.01547 ± 0.00011	0.013363 ± 0.000095	0.011136 ± 0.000079
Esophagus basal cells	0.01319 ± 0.00064	0.01204 ± 0.00059	0.01085 ± 0.00054
Liver	0.020727 ± 0.000027	0.018583 ± 0.000024	0.016756 ± 0.00002
Thyroid	0.01179 ± 0.00015	0.00991 ± 0.00013	0.00819 ± 0.00011
50um endosteal region (endosteal cells)	0.010297 ± 0.000013	0.008808 ± 0.000011	0.0072138 ± 0.0000091
Brain	0.034933 ± 0.000042	0.034069 ± 0.000041	0.032807 ± 0.000039
Salivary glands	0.011605 ± 0.000082	0.009676 ± 0.00007	0.007841 ± 0.00006
Skin	0.008833 ± 0.000011	0.0072457 ± 0.0000097	0.0055504 ± 0.0000074
Basal cells of skin	0.007097 ± 0.000028	0.005917 ± 0.000025	0.00457 ± 0.00002
Right adrenal + left adrenal	0.01465 ± 0.00018	0.01278 ± 0.00016	0.0104 ± 0.00013
ET region	0.01197 ± 0.00015	0.0103 ± 0.00013	0.00833 ± 0.00011
Gallbladder wall	0.01435 ± 0.00023	0.01251 ± 0.00019	0.01103 ± 0.00017
Heart wall	0.06903 ± 0.00011	0.060533 ± 0.000097	0.053162 ± 0.000085
Right kidney + left kidney	0.013239 ± 0.000038	0.011373 ± 0.000033	0.009306 ± 0.000027
Systemic lymph nodes	0.01462 ± 0.000059	0.012566 ± 0.000051	0.010473 ± 0.000042

Muscle	0.011407 ± 0.0000046	0.0095569 ± 0.0000048	0.0076501 ± 0.0000038
Oral mucosa	0.01047 ± 0.0006	0.00935 ± 0.00055	0.00741 ± 0.00045
Pancreas	0.013655 ± 0.000063	0.011765 ± 0.000054	0.009938 ± 0.000045
Prostate	--	--	--
Small intestine wall	0.015152 ± 0.000028	0.013047 ± 0.000024	0.011025 ± 0.000021
Stem cells of small intestine	0.0142 ± 0.0002	0.01228 ± 0.00018	0.01046 ± 0.00015
Spleen	0.012806 ± 0.000055	0.011071 ± 0.000048	0.009014 ± 0.000039
Thymus	0.01408 ± 0.00016	0.01207 ± 0.00014	0.01025 ± 0.00011
Uterus/cervix	0.02905 ± 0.00011	0.025108 ± 0.000098	0.021279 ± 0.000083
Tongue	0.011754 ± 0.000091	0.009838 ± 0.000077	0.007934 ± 0.000065
Tonsils	0.01209 ± 0.00038	0.00999 ± 0.00032	0.00825 ± 0.00027
Right colon wall (ascending + right transverse)	0.012634 ± 0.000051	0.010905 ± 0.000044	0.009418 ± 0.000037
Left colon wall (left transverse + descending)	0.012835 ± 0.000052	0.010975 ± 0.000045	0.009278 ± 0.000037
Rectosigmoid colon wall (sigmoid + rectum)	0.02044 ± 0.00011	0.017508 ± 0.000091	0.014668 ± 0.000076
Stem cells of right colon (ascending + right transverse)	0.01184 ± 0.00033	0.00938 ± 0.00027	0.00926 ± 0.00026
Stem cells of left colon (left transverse + descending)	0.01255 ± 0.00042	0.00985 ± 0.00036	0.00906 ± 0.00032
Stem cells of rectosigmoid colon (sigmoid + rectum)	0.02056 ± 0.00063	0.01682 ± 0.00052	0.01427 ± 0.00044
Basal cells of anterior nasal passages	0.0079 ± 0.0016	0.0124 ± 0.0023	0.0054 ± 0.0012
Basal cells of posterior nasal passages + pharynx	0.0212 ± 0.0023	0.015 ± 0.0016	0.014 ± 0.0015
Extrathoracic lymph nodes	0.01292 ± 0.00019	0.01144 ± 0.00017	0.00921 ± 0.00014
Bronchial basal cells	0.0192 ± 0.0014	0.0146 ± 0.0011	0.01349 ± 0.00096
Bronchial secretory cells	0.0199 ± 0.0014	0.0154 ± 0.0012	0.0149 ± 0.0011
Bronchiolar secretory cells	--	--	--
Alveolar-interstitium	0.021473 ± 0.000032	0.019091 ± 0.000028	0.016812 ± 0.000025
Thoracic lymph nodes	0.01377 ± 0.00019	0.01216 ± 0.00016	0.00986 ± 0.00013
Right lung lobe	0.021398 ± 0.000043	0.019002 ± 0.000038	0.016799 ± 0.000034
Left lung lobe	0.021565 ± 0.000047	0.0192 ± 0.000042	0.016828 ± 0.000037
Right adrenal gland	0.01466 ± 0.00025	0.01271 ± 0.00021	0.01015 ± 0.00017

Left adrenal gland	0.01463 ± 0.00027	0.01287 ± 0.00024	0.0107 ± 0.0002
Right breast adipose	0.01171 ± 0.000061	0.009774 ± 0.000046	0.008345 ± 0.000033
Right breast glandular	0.011909 ± 0.000071	0.010096 ± 0.000061	0.008354 ± 0.00005
Left breast adipose	0.012213 ± 0.000062	0.010399 ± 0.000048	0.008519 ± 0.000033
Left breast glandular	0.012705 ± 0.000074	0.010872 ± 0.000062	0.008971 ± 0.000052
Right breast (adipose + glandular)	0.011798 ± 0.000046	0.009898 ± 0.000037	0.008348 ± 0.000028
Left breast (adipose + glandular)	0.012431 ± 0.000048	0.010581 ± 0.000038	0.008657 ± 0.000028
Breast (adipose)	0.01171 ± 0.000043	0.009774 ± 0.000032	0.008345 ± 0.000024
Breast (glandular)	0.011909 ± 0.000051	0.010096 ± 0.000043	0.008354 ± 0.000035
Entire lenses of eye	0.01234 ± 0.00095	0.00791 ± 0.0007	0.00532 ± 0.00055
Sensitive lenses of eye	0.01 ± 0.0018	0.0081 ± 0.0015	0.0046 ± 0.0013
Right kidney cortex	0.013566 ± 0.000066	0.011589 ± 0.000057	0.009633 ± 0.000047
Right kidney medulla	0.01362 ± 0.00013	0.01171 ± 0.00011	0.009849 ± 0.000091
Right kidney pelvis	0.01353 ± 0.00027	0.01209 ± 0.00024	0.00977 ± 0.00019
Right kidney (cortex + medulla + pelvis)	0.013576 ± 0.000058	0.011631 ± 0.000049	0.00968 ± 0.000041
Left kidney cortex	0.012865 ± 0.00006	0.011054 ± 0.000051	0.008871 ± 0.000042
Left kidney medulla	0.01276 ± 0.00011	0.010996 ± 0.000097	0.00898 ± 0.00008
Left kidney pelvis	0.01289 ± 0.00025	0.01107 ± 0.00021	0.00897 ± 0.00017
Left kidney (cortex + medulla + pelvis)	0.012845 ± 0.000052	0.011043 ± 0.000044	0.008896 ± 0.000036
Right ovary	0.0209 ± 0.00033	0.0176 ± 0.00028	0.01455 ± 0.00023
Left ovary	0.02142 ± 0.00033	0.01868 ± 0.00029	0.01542 ± 0.00024
Pituitary gland	0.01925 ± 0.00099	0.01849 ± 0.00095	0.01614 ± 0.00083
Spinal cord	0.01275 ± 0.00015	0.01137 ± 0.00013	0.00891 ± 0.00011
Ureters	0.01607 ± 0.00019	0.01424 ± 0.00016	0.01173 ± 0.00013
Adipose/residual tissue	0.011153 ± 0.0000045	0.0092322 ± 0.0000037	0.007372 ± 0.0000022
Total body	0.0129123 ± 0.0000031	0.0107934 ± 0.0000028	0.0086145 ± 0.000002
e_{DW} or e (mSv/MBq)	0.0207713 ± 0.0000033	0.0179528 ± 0.0000025	0.0153921 ± 0.0000019

Supplementary Table S6: ^{18}F-FDG organ-level absorbed dose coefficients (mGy/MBq) for the 10th percentile standing height adult male PSPs.

Organ/tissue	Absorbed dose coefficient (mGy/MBq)		
	H10 / W10 male (167 cm / 55.9 kg)	H10 / W50 male (167 cm / 70.6 kg)	H10 / W90 male (167 cm / 90.2 kg)
Red (active) marrow	0.012844 ± 0.000015	0.011025 ± 0.000013	0.009494 ± 0.000011
Colon wall	0.014117 ± 0.000036	0.012369 ± 0.000031	0.010661 ± 0.000026
Stem cells of colon	0.01322 ± 0.00027	0.01158 ± 0.00023	0.00984 ± 0.0002
Right lung + left lung	0.021109 ± 0.000031	0.018558 ± 0.000027	0.016574 ± 0.000025
Stomach wall	0.014527 ± 0.000058	0.012472 ± 0.000048	0.010783 ± 0.000042
Stem cells of stomach	0.01258 ± 0.00032	0.01079 ± 0.00028	0.0093 ± 0.00024
Breast adipose + breast glandular	0.01084 ± 0.00015	0.00946 ± 0.00012	0.007787 ± 0.000086
Right ovary + left ovary	--	--	--
Testes	0.01164 ± 0.00012	0.01033 ± 0.00011	0.008331 ± 0.000089
Urinary bladder wall	0.05952 ± 0.00021	0.05232 ± 0.00018	0.04675 ± 0.00016
Urinary bladder basal cells	0.1155 ± 0.001	0.10054 ± 0.00089	0.08814 ± 0.00079
Esophagus wall	0.0161 ± 0.00011	0.013909 ± 0.000098	0.011764 ± 0.000082
Esophagus basal cells	0.01451 ± 0.00073	0.01101 ± 0.0006	0.01188 ± 0.00062
Liver	0.020451 ± 0.000025	0.018144 ± 0.000022	0.01643 ± 0.00002
Thyroid	0.01184 ± 0.00016	0.00994 ± 0.00013	0.00822 ± 0.00011
50um endosteal region (endosteal cells)	0.010705 ± 0.000012	0.0090691 ± 0.0000099	0.0076746 ± 0.0000085
Brain	0.03391 ± 0.000041	0.032878 ± 0.000039	0.031709 ± 0.000038
Salivary glands	0.011101 ± 0.000077	0.009283 ± 0.000066	0.007567 ± 0.000056
Skin	0.008959 ± 0.00001	0.0072862 ± 0.0000084	0.0058335 ± 0.0000073
Basal cells of skin	0.007113 ± 0.000028	0.005811 ± 0.000024	0.004771 ± 0.000021
Right adrenal + left adrenal	0.01547 ± 0.00019	0.01329 ± 0.00016	0.01084 ± 0.00014
ET region	0.01156 ± 0.00011	0.00974 ± 0.000093	0.00819 ± 0.000081
Gallbladder wall	0.01459 ± 0.00022	0.01295 ± 0.00019	0.01151 ± 0.00017
Heart wall	0.06487 ± 0.0001	0.0564 ± 0.00009	0.05 ± 0.00008
Right kidney + left kidney	0.013542 ± 0.000039	0.011587 ± 0.000033	0.00987 ± 0.000028
Systemic lymph nodes	0.015907 ± 0.000061	0.013696 ± 0.000052	0.011844 ± 0.000044

Muscle	0.011284 ± 0.0000045	0.0094595 ± 0.0000038	0.0078654 ± 0.0000031
Oral mucosa	0.01094 ± 0.00059	0.01004 ± 0.00055	0.00758 ± 0.00045
Pancreas	0.014879 ± 0.000067	0.012685 ± 0.000056	0.010869 ± 0.000048
Prostate	0.0274 ± 0.00025	0.02483 ± 0.00022	0.0219 ± 0.00019
Small intestine wall	0.014777 ± 0.000029	0.012693 ± 0.000024	0.011018 ± 0.000021
Stem cells of small intestine	0.01356 ± 0.0002	0.01152 ± 0.00017	0.01018 ± 0.00015
Spleen	0.013507 ± 0.000057	0.011467 ± 0.000048	0.009712 ± 0.000041
Thymus	0.01381 ± 0.00016	0.012 ± 0.00013	0.01015 ± 0.00011
Uterus/cervix	--	--	--
Tongue	0.011388 ± 0.000085	0.009539 ± 0.000073	0.007879 ± 0.000062
Tonsils	0.01369 ± 0.00042	0.01141 ± 0.00036	0.01029 ± 0.00032
Right colon wall (ascending + right transverse)	0.012808 ± 0.000054	0.011121 ± 0.000046	0.009653 ± 0.000039
Left colon wall (left transverse + descending)	0.012001 ± 0.000053	0.010225 ± 0.000045	0.008719 ± 0.000038
Rectosigmoid colon wall (sigmoid + rectum)	0.0192 ± 0.00012	0.016389 ± 0.000099	0.014234 ± 0.000086
Stem cells of right colon (ascending + right transverse)	0.01166 ± 0.00039	0.01061 ± 0.00034	0.00892 ± 0.0003
Stem cells of left colon (left transverse + descending)	0.01146 ± 0.00044	0.00962 ± 0.00036	0.00804 ± 0.00031
Stem cells of rectosigmoid colon (sigmoid + rectum)	0.01791 ± 0.0006	0.01558 ± 0.00052	0.01357 ± 0.00046
Basal cells of anterior nasal passages	0.0091 ± 0.0011	0.0064 ± 0.00088	0.00575 ± 0.00087
Basal cells of posterior nasal passages + pharynx	0.0193 ± 0.0014	0.015 ± 0.0011	0.0149 ± 0.0012
Extrathoracic lymph nodes	0.01285 ± 0.00018	0.01092 ± 0.00016	0.00936 ± 0.00014
Bronchial basal cells	0.0196 ± 0.001	0.01615 ± 0.00087	0.01428 ± 0.00077
Bronchial secretory cells	0.0201 ± 0.001	0.01623 ± 0.00086	0.01354 ± 0.00073
Bronchiolar secretory cells	--	--	--
Alveolar-interstitium	0.021109 ± 0.000031	0.018558 ± 0.000027	0.016574 ± 0.000025
Thoracic lymph nodes	0.01435 ± 0.00019	0.0126 ± 0.00016	0.01064 ± 0.00014
Right lung lobe	0.021013 ± 0.000042	0.018512 ± 0.000037	0.016573 ± 0.000033
Left lung lobe	0.021223 ± 0.000047	0.018614 ± 0.000041	0.016575 ± 0.000036
Right adrenal gland	0.01547 ± 0.00027	0.01329 ± 0.00023	0.01084 ± 0.00019

Left adrenal gland	0.014 ± 0.00026	0.01203 ± 0.00022	0.01 ± 0.00019
Right breast adipose	0.01095 ± 0.00029	0.0097 ± 0.00021	0.00794 ± 0.00015
Right breast glandular	0.01072 ± 0.00032	0.00904 ± 0.00026	0.00742 ± 0.00022
Left breast adipose	0.01154 ± 0.00029	0.00949 ± 0.00021	0.0081 ± 0.00015
Left breast glandular	0.0103 ± 0.0003	0.00855 ± 0.00026	0.00701 ± 0.00022
Right breast (adipose + glandular)	0.01084 ± 0.00021	0.00946 ± 0.00017	0.00779 ± 0.00012
Left breast (adipose + glandular)	0.01096 ± 0.00021	0.00913 ± 0.00016	0.00778 ± 0.00012
Breast (adipose)	0.01095 ± 0.00021	0.0097 ± 0.00015	0.00794 ± 0.0001
Breast (glandular)	0.01072 ± 0.00022	0.00904 ± 0.00019	0.00742 ± 0.00016
Entire lenses of eye	0.00977 ± 0.00085	0.00785 ± 0.00072	0.00858 ± 0.00078
Sensitive lenses of eye	0.0151 ± 0.0024	0.0063 ± 0.0011	0.0115 ± 0.0019
Right kidney cortex	0.013765 ± 0.000065	0.011823 ± 0.000054	0.010116 ± 0.000047
Right kidney medulla	0.01396 ± 0.00013	0.0121 ± 0.00011	0.010542 ± 0.000094
Right kidney pelvis	0.01397 ± 0.00027	0.01252 ± 0.00024	0.01044 ± 0.0002
Right kidney (cortex + medulla + pelvis)	0.013808 ± 0.000057	0.011899 ± 0.000048	0.010206 ± 0.000041
Left kidney cortex	0.013012 ± 0.000064	0.011093 ± 0.000054	0.009369 ± 0.000046
Left kidney medulla	0.01352 ± 0.00013	0.01124 ± 0.00011	0.009503 ± 0.00009
Left kidney pelvis	0.01334 ± 0.00028	0.01163 ± 0.00024	0.00969 ± 0.0002
Left kidney (cortex + medulla + pelvis)	0.013117 ± 0.000056	0.011139 ± 0.000047	0.009405 ± 0.00004
Right ovary	--	--	--
Left ovary	--	--	--
Pituitary gland	0.0194 ± 0.001	0.01678 ± 0.00094	0.01457 ± 0.00083
Spinal cord	0.01318 ± 0.00012	0.01108 ± 0.0001	0.009424 ± 0.000088
Ureters	0.0172 ± 0.0002	0.0149 ± 0.00017	0.01303 ± 0.00015
Adipose/residual tissue	0.012027 ± 0.000006	0.0096353 ± 0.0000039	0.0078054 ± 0.0000031
Total body	0.0130624 ± 0.0000033	0.0108538 ± 0.0000026	0.0090067 ± 0.0000022
e_{DW} or e (mSv/MBq)	0.0199197 ± 0.0000048	0.0172916 ± 0.0000037	0.0150214 ± 0.0000028

Supplementary Table S7: ^{18}F-FDG organ-level absorbed dose coefficients (mGy/MBq) for the 50th percentile standing height adult male PSPs.

Organ/tissue	Absorbed dose coefficient (mGy/MBq)		
	H50 / W10 male (177 cm / 64.7 kg)	H50 / W50 male (177 cm / 79.3 kg)	H50 / W90 male (177 cm / 99.1 kg)
Red (active) marrow	0.011418 ± 0.000013	0.009979 ± 0.000011	0.0087713 ± 0.0000099
Colon wall	0.012845 ± 0.000032	0.011242 ± 0.000028	0.009499 ± 0.000023
Stem cells of colon	0.01212 ± 0.00024	0.01041 ± 0.00021	0.00864 ± 0.00018
Right lung + left lung	0.018779 ± 0.000028	0.016733 ± 0.000025	0.015106 ± 0.000022
Stomach wall	0.012878 ± 0.000051	0.011252 ± 0.000044	0.009824 ± 0.000038
Stem cells of stomach	0.01046 ± 0.00028	0.00967 ± 0.00025	0.00858 ± 0.00022
Breast adipose + breast glandular	0.00966 ± 0.00013	0.00847 ± 0.0001	0.00701 ± 0.000078
Right ovary + left ovary	--	--	--
Testes	0.01046 ± 0.00011	0.008788 ± 0.000092	0.007624 ± 0.00008
Urinary bladder wall	0.05359 ± 0.00019	0.04784 ± 0.00016	0.04298 ± 0.00015
Urinary bladder basal cells	0.10104 ± 0.00091	0.08985 ± 0.0008	0.07976 ± 0.00072
Esophagus wall	0.01434 ± 0.0001	0.012617 ± 0.000087	0.010752 ± 0.000074
Esophagus basal cells	0.01481 ± 0.00071	0.01219 ± 0.00063	0.00967 ± 0.00051
Liver	0.018226 ± 0.000022	0.016422 ± 0.00002	0.014934 ± 0.000018
Thyroid	0.01003 ± 0.00013	0.00875 ± 0.00012	0.00774 ± 0.0001
50um endosteal region (endosteal cells)	0.009515 ± 0.00001	0.0079932 ± 0.0000089	0.0068931 ± 0.0000077
Brain	0.032571 ± 0.000039	0.031604 ± 0.000038	0.030585 ± 0.000037
Salivary glands	0.009688 ± 0.000069	0.008232 ± 0.00006	0.00697 ± 0.000052
Skin	0.0079062 ± 0.0000092	0.0064697 ± 0.0000075	0.0053954 ± 0.0000068
Basal cells of skin	0.006194 ± 0.000025	0.005229 ± 0.000022	0.004347 ± 0.000019
Right adrenal + left adrenal	0.01345 ± 0.00017	0.01151 ± 0.00014	0.01027 ± 0.00013
ET region	0.010144 ± 0.000095	0.00873 ± 0.000085	0.007572 ± 0.000075
Gallbladder wall	0.01303 ± 0.0002	0.01166 ± 0.00017	0.0103 ± 0.00015
Heart wall	0.057359 ± 0.000092	0.050815 ± 0.000081	0.04553 ± 0.000073
Right kidney + left kidney	0.011979 ± 0.000035	0.010421 ± 0.00003	0.009009 ± 0.000026
Systemic lymph nodes	0.014063 ± 0.000053	0.012327 ± 0.000046	0.010868 ± 0.00004

Muscle	0.0099572 ± 0.000004	0.0085128 ± 0.0000034	0.0072307 ± 0.0000029
Oral mucosa	0.00999 ± 0.00053	0.00862 ± 0.00049	0.00721 ± 0.00042
Pancreas	0.013128 ± 0.000058	0.011445 ± 0.00005	0.009859 ± 0.000043
Prostate	0.02484 ± 0.00023	0.02217 ± 0.0002	0.02 ± 0.00018
Small intestine wall	0.013035 ± 0.000024	0.011482 ± 0.000021	0.009989 ± 0.000019
Stem cells of small intestine	0.01176 ± 0.00017	0.01066 ± 0.00016	0.00928 ± 0.00014
Spleen	0.011918 ± 0.00005	0.010315 ± 0.000043	0.008893 ± 0.000037
Thymus	0.01207 ± 0.00014	0.01061 ± 0.00012	0.00929 ± 0.0001
Uterus/cervix	--	--	--
Tongue	0.010167 ± 0.000077	0.008711 ± 0.000068	0.007206 ± 0.000058
Tonsils	0.01271 ± 0.00039	0.01144 ± 0.00035	0.00926 ± 0.0003
Right colon wall (ascending + right transverse)	0.011455 ± 0.000048	0.010087 ± 0.000042	0.008719 ± 0.000036
Left colon wall (left transverse + descending)	0.010578 ± 0.000047	0.009258 ± 0.000041	0.00786 ± 0.000034
Rectosigmoid colon wall (sigmoid + rectum)	0.01743 ± 0.00011	0.015117 ± 0.00009	0.013245 ± 0.000079
Stem cells of right colon (ascending + right transverse)	0.01078 ± 0.00034	0.00963 ± 0.00032	0.00806 ± 0.00027
Stem cells of left colon (left transverse + descending)	0.00989 ± 0.00038	0.00783 ± 0.0003	0.00684 ± 0.00027
Stem cells of rectosigmoid colon (sigmoid + rectum)	0.01704 ± 0.00056	0.0149 ± 0.0005	0.01182 ± 0.0004
Basal cells of anterior nasal passages	0.0095 ± 0.0011	0.0068 ± 0.0011	0.00519 ± 0.00076
Basal cells of posterior nasal passages + pharynx	0.0178 ± 0.0013	0.0143 ± 0.0011	0.01258 ± 0.00097
Extrathoracic lymph nodes	0.01182 ± 0.00017	0.01026 ± 0.00014	0.00884 ± 0.00013
Bronchial basal cells	0.01773 ± 0.00093	0.01382 ± 0.00074	0.01284 ± 0.00071
Bronchial secretory cells	0.01792 ± 0.00096	0.01378 ± 0.00074	0.0128 ± 0.00069
Bronchiolar secretory cells	--	--	--
Alveolar-interstitium	0.018779 ± 0.000028	0.016733 ± 0.000025	0.015106 ± 0.000022
Thoracic lymph nodes	0.01278 ± 0.00017	0.01128 ± 0.00014	0.01004 ± 0.00013
Right lung lobe	0.018719 ± 0.000037	0.016698 ± 0.000033	0.015101 ± 0.00003
Left lung lobe	0.01885 ± 0.000041	0.016775 ± 0.000037	0.015112 ± 0.000032
Right adrenal gland	0.01345 ± 0.00024	0.01151 ± 0.0002	0.01027 ± 0.00018

Left adrenal gland	0.01236 ± 0.00023	0.01036 ± 0.0002	0.00921 ± 0.00017
Right breast adipose	0.00992 ± 0.00024	0.00893 ± 0.00019	0.00724 ± 0.00013
Right breast glandular	0.00931 ± 0.00027	0.00769 ± 0.00023	0.00645 ± 0.00019
Left breast adipose	0.01036 ± 0.00024	0.00894 ± 0.00019	0.00709 ± 0.00013
Left breast glandular	0.00947 ± 0.00027	0.00713 ± 0.00022	0.00624 ± 0.00019
Right breast (adipose + glandular)	0.00966 ± 0.00018	0.00847 ± 0.00015	0.00701 ± 0.00011
Left breast (adipose + glandular)	0.00997 ± 0.00018	0.00827 ± 0.00014	0.00684 ± 0.00011
Breast (adipose)	0.00992 ± 0.00017	0.00893 ± 0.00013	0.007244 ± 0.000094
Breast (glandular)	0.00931 ± 0.00019	0.00769 ± 0.00016	0.00645 ± 0.00014
Entire lenses of eye	0.00872 ± 0.0008	0.00855 ± 0.00076	0.00665 ± 0.00064
Sensitive lenses of eye	0.0057 ± 0.0012	0.0085 ± 0.0016	0.0058 ± 0.0012
Right kidney cortex	0.012221 ± 0.000057	0.010633 ± 0.000049	0.009221 ± 0.000042
Right kidney medulla	0.01251 ± 0.00011	0.010988 ± 0.000098	0.00956 ± 0.000085
Right kidney pelvis	0.01232 ± 0.00024	0.01109 ± 0.00021	0.00952 ± 0.00018
Right kidney (cortex + medulla + pelvis)	0.012277 ± 0.00005	0.010716 ± 0.000043	0.009295 ± 0.000037
Left kidney cortex	0.011533 ± 0.000057	0.009948 ± 0.000049	0.008591 ± 0.000042
Left kidney medulla	0.0116 ± 0.00011	0.010177 ± 0.000096	0.008565 ± 0.000081
Left kidney pelvis	0.01167 ± 0.00024	0.0104 ± 0.00021	0.00874 ± 0.00018
Left kidney (cortex + medulla + pelvis)	0.011549 ± 0.000049	0.010007 ± 0.000043	0.008591 ± 0.000037
Right ovary	--	--	--
Left ovary	--	--	--
Pituitary gland	0.01857 ± 0.001	0.01595 ± 0.00089	0.01588 ± 0.00084
Spinal cord	0.01169 ± 0.00011	0.010053 ± 0.000093	0.008673 ± 0.000081
Ureters	0.01522 ± 0.00018	0.01332 ± 0.00015	0.01185 ± 0.00013
Adipose/residual tissue	0.010387 ± 0.0000052	0.0086155 ± 0.0000034	0.0071031 ± 0.0000028
Total body	0.0114761 ± 0.0000029	0.0100548 ± 0.0000027	0.0082201 ± 0.000002
e_{DW} or e (mSv/MBq)	0.0176694 ± 0.0000037	0.0155005 ± 0.0000029	0.0136077 ± 0.0000023

Supplementary Table S8: ^{18}F-FDG organ-level absorbed dose coefficients (mGy/MBq) for the 90th percentile standing height adult male PSPs.

Organ/tissue	Absorbed dose coefficient (mGy/MBq)		
	H90 / W10 male (186 cm / 74.2 kg)	H90 / W50 male (186 cm / 88.7 kg)	H90 / W90 male (186 cm / 108.4 kg)
Red (active) marrow	0.010275 ± 0.000012	0.009148 ± 0.00001	0.0080557 ± 0.0000091
Colon wall	0.011337 ± 0.000028	0.010188 ± 0.000025	0.009039 ± 0.000022
Stem cells of colon	0.01078 ± 0.00021	0.00938 ± 0.00019	0.00871 ± 0.00018
Right lung + left lung	0.016896 ± 0.000025	0.015254 ± 0.000022	0.013866 ± 0.00002
Stomach wall	0.011584 ± 0.000045	0.010266 ± 0.00004	0.009161 ± 0.000035
Stem cells of stomach	0.00987 ± 0.00026	0.00895 ± 0.00023	0.00818 ± 0.00021
Breast adipose + breast glandular	0.00855 ± 0.00011	0.007463 ± 0.000089	0.006578 ± 0.000072
Right ovary + left ovary	--	--	--
Testes	0.009482 ± 0.000097	0.008087 ± 0.000084	0.007281 ± 0.000075
Urinary bladder wall	0.04822 ± 0.00016	0.04359 ± 0.00015	0.03967 ± 0.00013
Urinary bladder basal cells	0.08945 ± 0.00081	0.08046 ± 0.00072	0.07213 ± 0.00066
Esophagus wall	0.012929 ± 0.000089	0.011432 ± 0.000078	0.0099 ± 0.000068
Esophagus basal cells	0.01292 ± 0.00064	0.0114 ± 0.00057	0.0098 ± 0.0005
Liver	0.016395 ± 0.00002	0.014999 ± 0.000018	0.013796 ± 0.000017
Thyroid	0.00938 ± 0.00012	0.00805 ± 0.0001	0.00679 ± 0.00009
50um endosteal region (endosteal cells)	0.0082778 ± 0.0000092	0.0073133 ± 0.000008	0.006365 ± 0.0000071
Brain	0.031262 ± 0.000038	0.030414 ± 0.000036	0.029442 ± 0.000035
Salivary glands	0.008616 ± 0.000062	0.007558 ± 0.000055	0.006411 ± 0.000049
Skin	0.0068933 ± 0.000008	0.0058728 ± 0.0000068	0.0049031 ± 0.0000061
Basal cells of skin	0.005497 ± 0.000023	0.004761 ± 0.00002	0.004001 ± 0.000018
Right adrenal + left adrenal	0.01177 ± 0.00015	0.01089 ± 0.00013	0.0092 ± 0.00011
ET region	0.009213 ± 0.000087	0.008058 ± 0.000078	0.006954 ± 0.00007
Gallbladder wall	0.0118 ± 0.00018	0.01046 ± 0.00016	0.00963 ± 0.00014
Heart wall	0.051223 ± 0.000082	0.046046 ± 0.000074	0.041662 ± 0.000062
Right kidney + left kidney	0.010668 ± 0.000031	0.009477 ± 0.000027	0.00819 ± 0.000024
Systemic lymph nodes	0.012661 ± 0.000047	0.011409 ± 0.000042	0.010282 ± 0.000037

Muscle	0.0088422 ± 0.0000035	0.0077247 ± 0.0000031	0.0066393 ± 0.0000027
Oral mucosa	0.00843 ± 0.00046	0.00756 ± 0.00041	0.00647 ± 0.00037
Pancreas	0.011748 ± 0.000052	0.010397 ± 0.000045	0.00919 ± 0.00004
Prostate	0.02236 ± 0.0002	0.02022 ± 0.00018	0.01869 ± 0.00016
Small intestine wall	0.011573 ± 0.000022	0.01041 ± 0.000019	0.009327 ± 0.000017
Stem cells of small intestine	0.01053 ± 0.00016	0.00974 ± 0.00014	0.00871 ± 0.00013
Spleen	0.010773 ± 0.000044	0.009362 ± 0.000038	0.00806 ± 0.000034
Thymus	0.01092 ± 0.00012	0.00973 ± 0.00011	0.00844 ± 0.000095
Uterus/cervix	--	--	--
Tongue	0.008992 ± 0.000069	0.007778 ± 0.000061	0.006726 ± 0.000054
Tonsils	0.01133 ± 0.00035	0.01028 ± 0.00032	0.00934 ± 0.0003
Right colon wall (ascending + right transverse)	0.010108 ± 0.000042	0.009102 ± 0.000037	0.00808 ± 0.000033
Left colon wall (left transverse + descending)	0.00939 ± 0.000041	0.008267 ± 0.000036	0.007381 ± 0.000032
Rectosigmoid colon wall (sigmoid + rectum)	0.01528 ± 0.000091	0.01382 ± 0.000081	0.01246 ± 0.000072
Stem cells of right colon (ascending + right transverse)	0.00974 ± 0.00032	0.00862 ± 0.00029	0.00808 ± 0.00027
Stem cells of left colon (left transverse + descending)	0.00934 ± 0.00035	0.00786 ± 0.0003	0.00713 ± 0.00027
Stem cells of rectosigmoid colon (sigmoid + rectum)	0.01425 ± 0.00048	0.0125 ± 0.00043	0.01172 ± 0.00039
Basal cells of anterior nasal passages	0.0078 ± 0.0011	0.0082 ± 0.001	0.00546 ± 0.00079
Basal cells of posterior nasal passages + pharynx	0.015 ± 0.0011	0.0147 ± 0.0011	0.0128 ± 0.001
Extrathoracic lymph nodes	0.01045 ± 0.00015	0.00929 ± 0.00013	0.00807 ± 0.00012
Bronchial basal cells	0.01587 ± 0.00081	0.01463 ± 0.00075	0.01218 ± 0.00067
Bronchial secretory cells	0.01553 ± 0.00082	0.01384 ± 0.00074	0.01256 ± 0.00067
Bronchiolar secretory cells	--	--	--
Alveolar-interstitium	0.016896 ± 0.000025	0.015254 ± 0.000022	0.013866 ± 0.00002
Thoracic lymph nodes	0.01164 ± 0.00015	0.01029 ± 0.00013	0.00886 ± 0.00011
Right lung lobe	0.016842 ± 0.000034	0.015216 ± 0.00003	0.013877 ± 0.000028
Left lung lobe	0.016961 ± 0.000037	0.0153 ± 0.000032	0.013853 ± 0.000029
Right adrenal gland	0.01177 ± 0.00021	0.01089 ± 0.00019	0.0092 ± 0.00016

Left adrenal gland	0.01046 ± 0.00019	0.00972 ± 0.00018	0.00813 ± 0.00015
Right breast adipose	0.00897 ± 0.00021	0.00781 ± 0.00016	0.00676 ± 0.00012
Right breast glandular	0.00798 ± 0.00023	0.00686 ± 0.0002	0.00615 ± 0.00018
Left breast adipose	0.00933 ± 0.00022	0.00784 ± 0.00016	0.00671 ± 0.00012
Left breast glandular	0.00881 ± 0.00025	0.00711 ± 0.0002	0.00622 ± 0.00018
Right breast (adipose + glandular)	0.00855 ± 0.00016	0.00746 ± 0.00013	0.00658 ± 0.0001
Left breast (adipose + glandular)	0.00911 ± 0.00016	0.00758 ± 0.00013	0.00657 ± 0.0001
Breast (adipose)	0.00897 ± 0.00015	0.00781 ± 0.00011	0.006758 ± 0.000087
Breast (glandular)	0.00798 ± 0.00016	0.00686 ± 0.00014	0.00615 ± 0.00013
Entire lenses of eye	0.00933 ± 0.00084	0.00797 ± 0.00076	0.00513 ± 0.00057
Sensitive lenses of eye	0.0081 ± 0.0014	0.0101 ± 0.002	0.00374 ± 0.00099
Right kidney cortex	0.010856 ± 0.00005	0.009698 ± 0.000045	0.008381 ± 0.000039
Right kidney medulla	0.01128 ± 0.0001	0.009902 ± 0.000088	0.008562 ± 0.000076
Right kidney pelvis	0.011 ± 0.00021	0.00999 ± 0.00019	0.00861 ± 0.00016
Right kidney (cortex + medulla + pelvis)	0.010939 ± 0.000044	0.009746 ± 0.000039	0.008423 ± 0.000034
Left kidney cortex	0.010254 ± 0.00005	0.009032 ± 0.000043	0.007798 ± 0.000038
Left kidney medulla	0.010231 ± 0.000096	0.009164 ± 0.000086	0.007987 ± 0.000075
Left kidney pelvis	0.01055 ± 0.00021	0.0096 ± 0.00019	0.00806 ± 0.00016
Left kidney (cortex + medulla + pelvis)	0.010261 ± 0.000044	0.009077 ± 0.000038	0.007842 ± 0.000033
Right ovary	--	--	--
Left ovary	--	--	--
Pituitary gland	0.01703 ± 0.00092	0.01524 ± 0.00084	0.01487 ± 0.00081
Spinal cord	0.01059 ± 0.000096	0.009073 ± 0.000083	0.007932 ± 0.000074
Ureters	0.01363 ± 0.00016	0.01232 ± 0.00014	0.01085 ± 0.00012
Adipose/residual tissue	0.0092199 ± 0.0000046	0.0078156 ± 0.0000031	0.0066291 ± 0.0000027
Total body	0.0102291 ± 0.0000026	0.0088606 ± 0.0000021	0.0075807 ± 0.0000018
e_{DW} or e (mSv/MBq)	0.0158446 ± 0.0000029	0.0141068 ± 0.0000024	0.0127004 ± 0.0000019